



## N-Propargylamine-hydroxypyridinone hybrids as multitarget agents for the treatment of Alzheimer's disease

Jianan Guo<sup>a</sup>, Yujia Zhang<sup>a</sup>, Changjun Zhang<sup>b</sup>, Chuansheng Yao<sup>a</sup>, Jingqi Zhang<sup>a</sup>, Xiaoying Jiang<sup>c</sup>, Zhichao Zhong<sup>a</sup>, Jiamin Ge<sup>a</sup>, Tao Zhou<sup>d</sup>, Renren Bai<sup>e,f,\*</sup>, Yuanyuan Xie<sup>a,b,\*</sup>

<sup>a</sup> College of Pharmaceutical Science, Zhejiang University of Technology, Hangzhou, PR China

<sup>b</sup> Collaborative Innovation Centre of Yangtze River Delta Region Green Pharmaceuticals, Zhejiang University of Technology, Hangzhou, PR China

<sup>c</sup> College of Material Chemistry and Chemical Engineering, Hangzhou Normal University, Hangzhou, PR China

<sup>d</sup> School of Food Science and Biotechnology, Zhejiang Gongshang University, Hangzhou, PR China

<sup>e</sup> College of Pharmacy, School of Medicine, Hangzhou Normal University, Hangzhou, PR China

<sup>f</sup> Key Laboratory of Elemene Class Anti-Cancer Chinese Medicines, Engineering Laboratory of Development and Application of Traditional Chinese Medicines, Collaborative Innovation Center of Traditional Chinese Medicines of Zhejiang Province, Hangzhou Normal University, Hangzhou, PR China

### ARTICLE INFO

#### Keywords:

Alzheimer's disease  
Multitarget-directed ligands  
N-Propargylamine  
Hydroxypyridinone  
Monoamine oxidase B  
Iron-chelating

### ABSTRACT

AD is a progressive brain disorder. Because of the lack of remarkable single-target drugs against neurodegenerative disorders, the multitarget-directed ligand strategy has received attention as a promising therapeutic approach. Herein, we rationally designed twenty-nine hybrids of N-propargylamine-hydroxypyridinone. The designed hybrids possessed excellent iron-chelating activity ( $pFe^{3+} = 17.09-22.02$ ) and potent monoamine oxidase B inhibitory effects. Various biological evaluations of the optimal compound **6b** were performed step by step, including inhibition screening of monoamine oxidase ( $hMAO-B IC_{50} = 0.083 \pm 0.001 \mu M$ ,  $hMAO-A IC_{50} = 6.11 \pm 0.08 \mu M$ ;  $SI = 73.5$ ), prediction of blood-brain barrier permeability and mouse behavioral research. All of these favorable results proved that the N-propargylamine-hydroxypyridinone scaffold is a promising structure for the discovery of multitargeted ligands for AD therapy.

### 1. Introduction

Alzheimer's disease (AD) is a progressive brain disorder, and the primary patients are elderly individuals. According to estimates by the World Alzheimer's Association, approximately 50 million people suffered from dementia in 2019, and this number is expected to increase to 152 million by 2050 [1], with age being the greatest risk factor for this disease [2]. About 50 million people have dementia worldwide, with nearly 25% living in China. With the increasing number of people suffering from Alzheimer's disease, the cost of nursing care and demand for nursing staff have imposed a huge burden on society and patients' families [3], to make matters worse, this situation cannot be improved by delaying the survival time of patients through drugs. According to the analysis of the mathematical model by Kuca *et al.*, the research findings showed that the total cost of care for all AD patients would increase by 2080, which would extend the length of a person's stay in the mild,

moderate, or severe stage. In accordance with the latest results, AD has become the sixth leading cause of death in the United States [4]. Since the discovery of AD, tremendous advances have been made in investigations of its pathogenesis; however, scientists have not yet identified its nosogenesis or fully clarified its pathology. The accumulation of extracellular amyloid- $\beta$  ( $A\beta$ ) and the formation of intracellular neurofibrillary tangles containing hyperphosphorylated tau in the brain are the typical pathological hallmarks of this disease [5,6]. To date, five commercially available drugs have been used for the treatment of AD: galantamine, donepezil, memantine, rivastigmine and memantine combined with donepezil [7,8]. Regrettably, there are no drugs that can effectively prevent or cure the progression of AD.

At present, low permeability of the blood-brain barrier (BBB) is one of the important reasons that hamper the drug development process [9]. However, BBB permeability is one of the most vital indicators for measuring central nervous system (CNS) drugs. General CNS drugs often

\* Corresponding authors at: Key Laboratory for Green Pharmaceutical Technologies and Related Equipment of Ministry of Education, College of Pharmaceutical Sciences, Zhejiang University of Technology, Hangzhou 310014, PR China (Y. Xie). College of Pharmacy, School of Medicine, Hangzhou Normal University, Hangzhou 311121, PR China (R. Bai).

E-mail addresses: [renrenbai@126.com](mailto:renrenbai@126.com), [renrenbai@hznu.edu.cn](mailto:renrenbai@hznu.edu.cn) (R. Bai), [xyycz@zjut.edu.cn](mailto:xyycz@zjut.edu.cn) (Y. Xie).

<https://doi.org/10.1016/j.bioorg.2021.105013>

Received 29 March 2021; Received in revised form 19 May 2021; Accepted 20 May 2021

Available online 25 May 2021

0045-2068/© 2021 Elsevier Inc. All rights reserved.

have the following characteristics: i) molecular weight  $\leq 450$ ; ii) hydrogen bond donors  $\leq 5$ ; iii) hydrogen bond acceptor  $\leq 10$ ; iv) log octanol/water partition coefficient  $\leq 5$ ; v) topological polar surface area  $\leq 90$  [10]. There are also important criteria for evaluating whether a compound can cross the BBB. This problem was mainly solved through the rational design of molecules. In addition, nano drug delivery systems are also one of the key research areas in the future [11].

Monoamine oxidases (MAOs) are FAD-containing enzymes that are responsible for monoaminergic homeostasis and neurotransmission [12]. MAOs are mainly divided into two isoenzymes (monoamine oxidase type A (MAO-A) and monoamine oxidase type B (MAO-B)) according to the specificity of their substrates and inhibitors. MAO-B displays potent affinity for nonhydroxylated amines such as benzylamine and  $\beta$ -phenethylamine [13]. Upregulated MAO-B activity in the brain mainly occurs in glial cells associated with  $\beta$ , which is one of the characteristics of AD [14], and its catalyzed neurotoxic substances can cause neuronal damage [15,16]. Therefore, MAO-B has been widely discussed and studied in recent years as a target for AD treatment. The results of *in vitro* and *in vivo* models of neurodegenerative diseases have proven that *N*-propargylamine derivatives with MAO-B inhibitory activity could protect neurons from apoptosis caused by various injuries [17,18]. As an important pharmacophore, the extensively studied *N*-propargylamine fragment has been applied to the design of small molecules against neurodegenerative diseases, and tremendous progress has been made [19,20,21] (Fig. 1). Selegiline and rasagiline, bearing this *N*-propargylamine fragment, exhibit excellent MAO inhibitory activity and therefore act as monoamine oxidase inhibitors to treat neurodegenerative diseases. *N*-propargylamine derivatives also exhibited neuroprotective effects. In *in vitro* cell experiments had shown that it can improve the decrease in cell viability induced by MPP<sup>+</sup> and  $A\beta_{1-40}$  or  $A\beta_{1-42}$  [22]. In addition, researchers have made different attempts to replace the *N*-H in the *N*-propargylamine functional group, including substitution with aliphatic or aromatic hydrocarbons [23,24]. We also used this idea as inspiration to modify the *N*-propargylamine functional group to expect more potential multitarget-directed ligands (MTDLs).

Iron is a crucial biometal for all life, is involved in a variety of biological activities and is utilized for neurotransmitter synthesis [25,26]. A plethora of evidence indicates that the dysregulation of neuronal iron is critical to the course of AD [27]. Recent investigations have also proved that iron ions are associated with the degree of amyloid deposition, and MRI studies have confirmed this idea [27,28,29]. Additionally, reactive oxygen species (ROS) are generated through catalysis by a high concentration of redox-active metal ions through the Fenton or Haber Weiss reactions, leading to oxidative stress and the death of nerve cells [30]. More importantly, the hydroxypyridinone core displays a high affinity

for iron ions, so its structural modification has been extensively investigated. Representatively, deferiprone (DFP) was approved by the FDA in 2011 as an iron chelator [31], and CN128 has been shown in recent years to be a compound with promising druggability (Fig. 1) [32]. Because of its good oral bioavailability, low glucuronidation and oxidation rates, and potent iron-chelating ability, hydroxypyridinone is currently in clinical trials for  $\beta$ -thalassemia. Moreover, the hydroxypyridinone core (with modification at positions 1 or 6) has the advantage of easy to modification and is considered to be a lead compound for the design of MTDLs for the treatment of AD [25,33].

The theory of “one molecule, one target, one disease” was widely circulated in the 20th century, but for neurodegenerative diseases, cardiovascular diseases and other multi-factor diseases, it was often failed to achieve people’s expected results by relying on a single target to develop new drugs. Hence, more and more attention has been paid to the therapies aimed at multiple targets to improve the therapeutic effect or safety. The MTDLs design strategy is the most promising. Its advantages are i) Overcoming the shortcomings of unclear pharmacokinetic (PK) properties during mixed administration; ii) In the case of low doses, it can also improve the therapeutic effect through synergy; iii) There is no drug-drug risk of interaction; iv) Simplify the dosing regimen Based on this strategy. We hope that through the rational design of the compounds, on the premise of inheriting the excellent iron-chelating ability of DFP, it can enhance its ability to penetrate the blood-brain barrier to achieve chelation of iron ions and inhibit MAO-B multi-targeting function in the brain [34,35].

Given the crucial roles of MAO-B and iron in AD, the design of MTDLs with both MAO-B and iron activity has aroused extensive attention in recent years [36,37,38,39]. M30, developed by Youdim *et al.*, is especially well known [19] (Fig. 1). Herein, *N*-propargylamine group and hydroxypyridone were selected as pharmacodynamic groups and pargyline was used as an important core for modification and transformation, so substitute benzyl as the main direction of exploration for *N*-substitutes. Form this, we designed a series of potentially active multifunctional hybrids and carried out further biological evaluations of the synthesized compounds (Fig. 2).

## 2. Results and discussion

### 2.1. Chemistry

The synthetic processes of compounds **6a-o** and **14a-n** are outlined in Schemes 1 and 2. Compounds **6a-o** were synthesized by a five-step reaction scheme using maltol as the raw material (Scheme 1). The synthetic methods of intermediate **3** were reported in our previous work

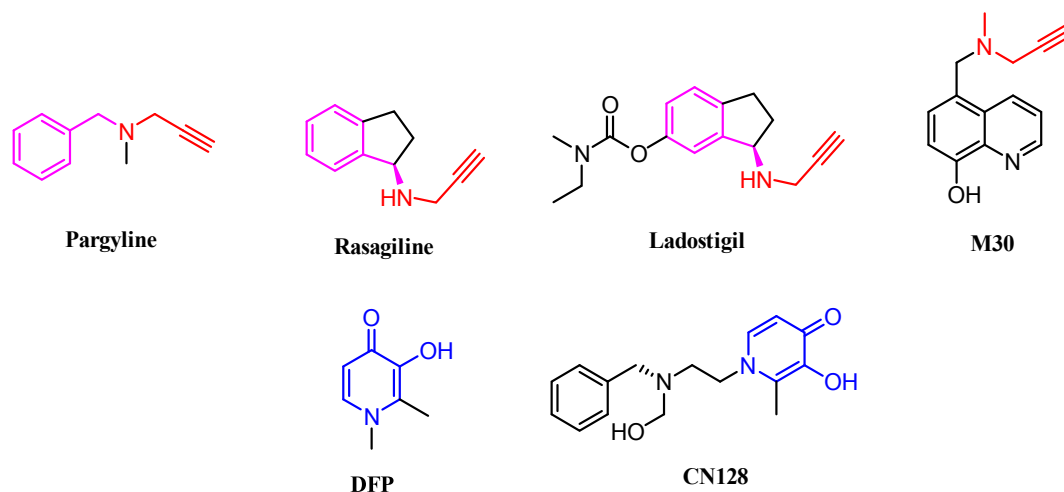


Fig. 1. Structures of representative *N*-propargylamine and hydroxypyridinone derivatives.

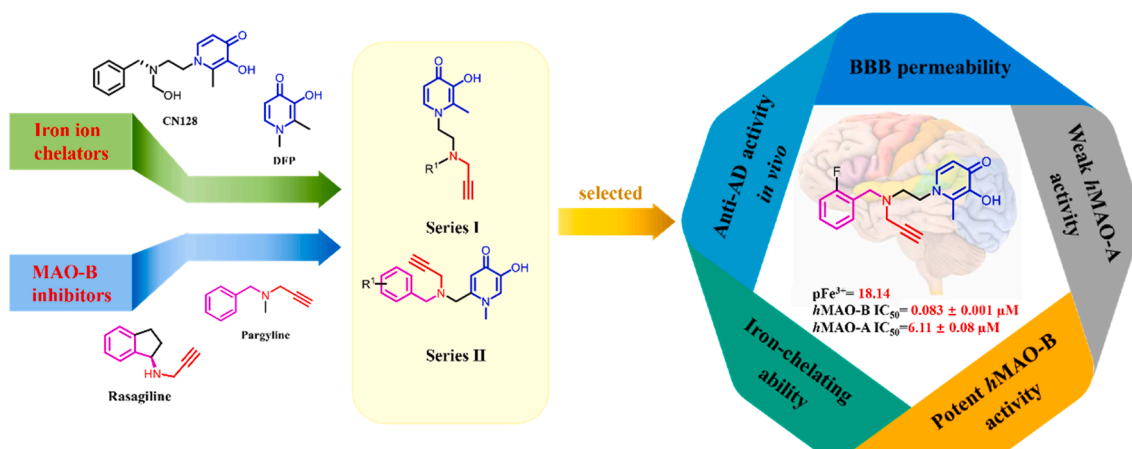
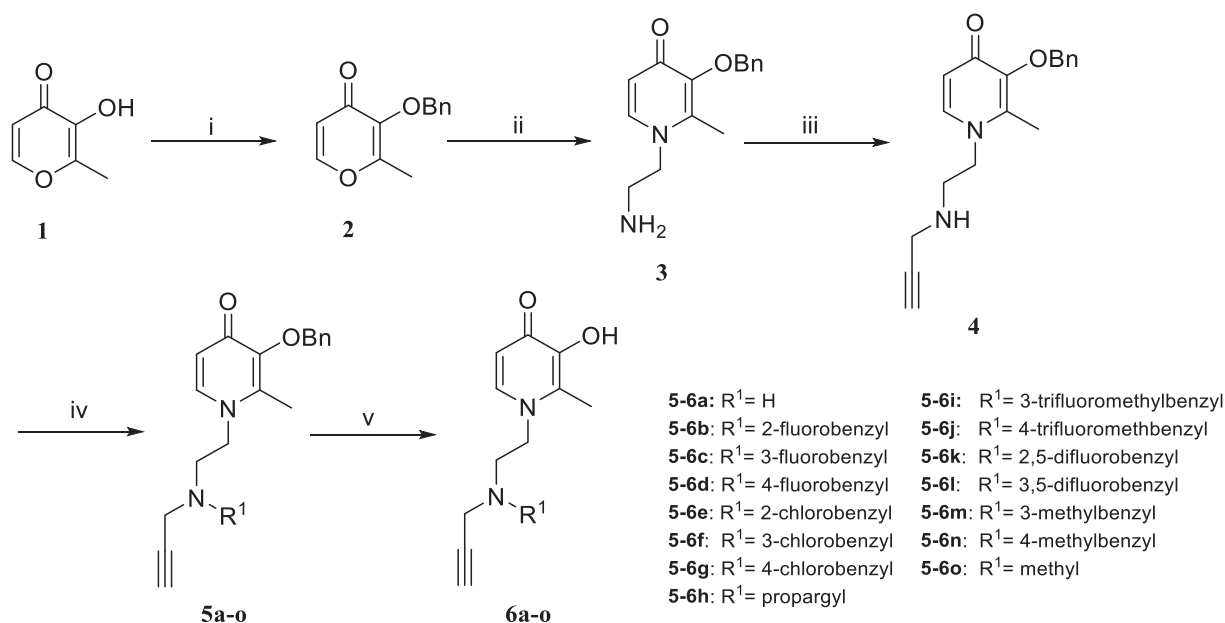


Fig. 2. Design strategy of *N*-propargylamine-hydroxypyridinone hybrids as potential anti-AD agents.



**Scheme 1.** Reagents and conditions: (i) benzyl bromide, K<sub>2</sub>CO<sub>3</sub>, acetone, reflux, 4 h; (ii) ethane-1,2-diamine, ethyl alcohol: H<sub>2</sub>O = 1:1, reflux, 1 h; (iii) 3-bromopropyne, K<sub>2</sub>CO<sub>3</sub>, DMF, r.t., 6 h; (iv) corresponding substituted benzyl bromides, methyl iodide or 3-bromopropyne, KOH, THF, reflux, 20 h. (v) BCl<sub>3</sub>, anhydrous DCM, -30 °C, 2 h.

[38]. Intermediate **4** was prepared by reacting compound **3** with 3-bromopropyne in DMF followed by undergoing a substitution reaction to obtain intermediates **5a-o**. Finally, **5a-o** reacted under nitrogen protection with boron trichloride to afford final products **6a-o**.

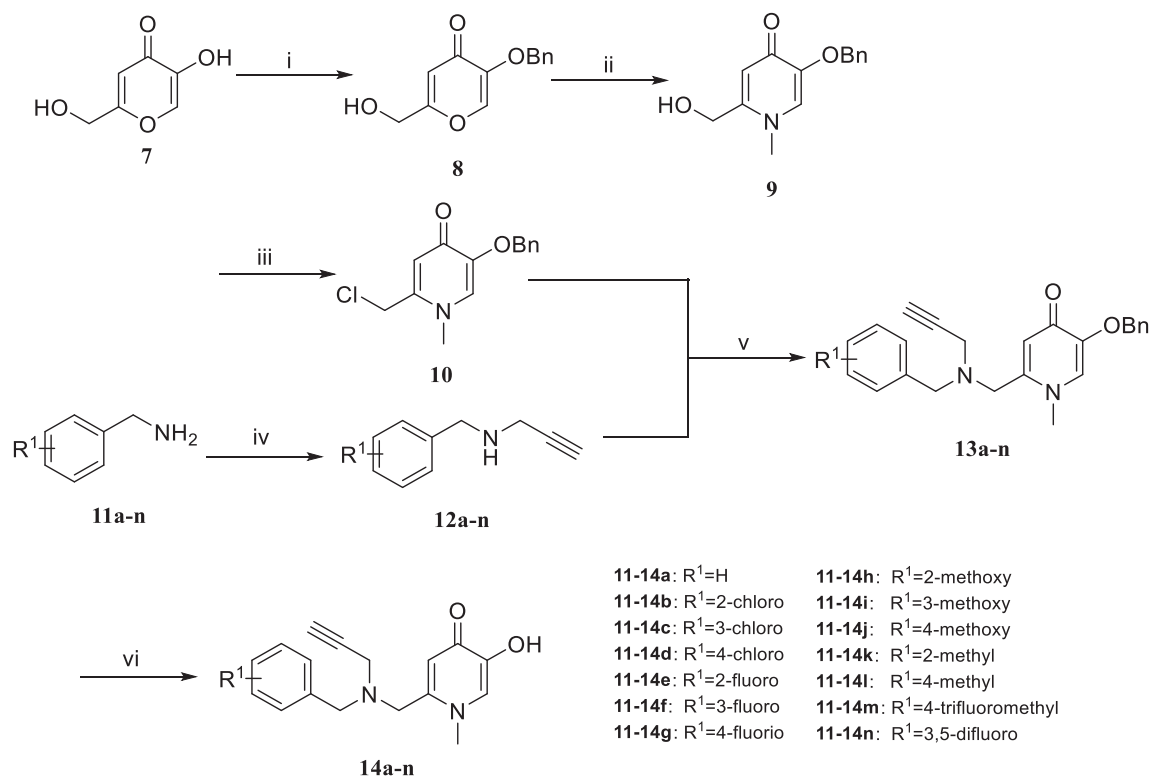
The synthesis process of compounds **14a-n** was divided into two parts (the synthesis of compound **10** and the preparation of intermediates **12a-n**) (Scheme 2). First, we used kojic acid as the raw material to prepare intermediate **10** by a three-step reaction. Intermediates **12a-n** were prepared via reaction of **11a-n** with 3-bromopropyne [40]. Then, intermediate **10** and intermediates **12a-n** were reacted with acetonitrile as the solvent and triethylamine as the acid-binding agent to obtain intermediates **13a-n**. Intermediates **13a-n** then underwent a deprotection reaction to afford the final products **14a-n**.

## 2.2. Iron-chelating ability assay

Because pyridone derivatives are bidentate ligands (3:1 complex) and their proton ionization characteristics (Fig. 3) [25], an automatic

spectrophotometric titration system was used to determine the pK<sub>a</sub> values and affinity constants for Fe<sup>3+</sup> of the hybrids. The results of all hybrids are listed in Table 1. All hybrids exhibited excellent iron-chelating activity (pFe<sup>3+</sup> = 17.09–22.02) (Table 1). Compound **14j** exerted the most potent iron-chelating effect (pFe<sup>3+</sup> = 22.02). Through comparison of the two series of compounds (compounds **6a-o** and **14a-n**), the compounds in series two were more capable of chelating Fe<sup>3+</sup> (pFe<sup>3+</sup> = 17.09–18.70 vs. pFe<sup>3+</sup> = 18.21–22.02).

The 3D UV spectrum of **6b** is shown below (pH = 1.3–11.0) (Fig. 4A), illustrating that compound **6b** has two pK<sub>a</sub> values: 3.65 (carbonyl) and 9.91 (phenol) (Fig. 4B). After repeating the titration in the pH range of 2.1–9.0, the visible spectrum shows the presence of FeL (corresponding constant: Log β<sub>1</sub>), FeL<sub>2</sub> (corresponding constant: Log β<sub>2</sub>) and FeL<sub>3</sub> (corresponding constant: Log β<sub>3</sub>) in the solution system. We, therefore, describe these three types of substances by measuring three equilibrium constants (compound **6b**): Log β<sub>1</sub> (14.37), Log β<sub>2</sub> (26.05) and Log β<sub>3</sub> (35.12) (Fig. 5A and Fig. 5B). The calculated pFe<sup>3+</sup> value of compound **6b** is 18.15. The abundance of each species of **6b** varied with pH, as shown in Fig. 5C. It can be seen from the above results that the hybrid we



**Scheme 2.** Reagents and conditions: (i) benzyl bromide, K<sub>2</sub>CO<sub>3</sub>, ethanol, reflux, 2 h; (ii) methylamine (40% in water), NaOH, ethyl alcohol:H<sub>2</sub>O = 1:1, reflux, 1 h; (iii) SOCl<sub>2</sub>, r.t., 1 h; (iv) 3-bromopropyne, K<sub>2</sub>CO<sub>3</sub>, DMF, 12 h (v) triethylamine, acetonitrile, reflux, 20 h. (vi) BCl<sub>3</sub>, anhydrous DCM, -20 °C, 2 h.

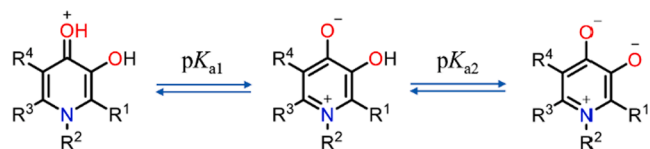


**Fig. 3.** Proton equilibria of pyridone derivatives.

designed fully inherited the characteristics of DFP chelation of iron ions and achieved the designed purpose.

### 2.3. hMAO-B/A inhibitory assay and selectivity

To verify the activity of the synthesized compounds against MAO-B, we conducted an *in vitro* hMAO-B activity assay. First, all hybrids were preliminarily screened at a concentration of 0.1 μM (Table 2), and then the compounds showing potent inhibitory effects were tested to determine their IC<sub>50</sub> values (Table 3).

From the results in Table 2, a total of ten hybrids exhibited inhibition >40%. Among them, compounds 6b and 6l showed excellent inhibitory activities compared with pargyline at a concentration of 0.1 μM (59 ± 2% and 50 ± 2%, respectively, vs. 50 ± 3%). Finally, these ten hybrid compounds with > 40% inhibition were selected and their specific IC<sub>50</sub> values were determined (Table 3).

According to the results in Table 3, the IC<sub>50</sub> values of the ten hybrids were all at the nanomolar level. In particular, compound Compound 6b demonstrated potent MAO-B inhibitory activity (IC<sub>50</sub> = 0.083 ± 0.001 μM), which was more active than pargyline (IC<sub>50</sub> = 0.097 ± 0.004 μM). Eventually, combining analysis results of Table 2 those in with Table 3, the framework of the series one compounds (6a-o) displayed more potent MAO-B inhibitory activity.

To further explore the inhibitory activity of the hybrids for the MAO-A subtype, the selectivity index for MAO-B was determined [selectivity index (SI): IC<sub>50</sub> (hMAO-A)/IC<sub>50</sub> (hMAO-B)]. As illustrated in Table 4,

**Table 1**

Acidity constants of the compounds and stability constants of the respective iron chelators.

Compound	pK <sub>a1</sub> <sup>a</sup>	pK <sub>a2</sub> <sup>a</sup>	Log β <sub>1</sub> <sup>c</sup>	Log β <sub>2</sub> <sup>c</sup>	Log β <sub>3</sub> <sup>c</sup>	pFe <sup>3+</sup>
6a	3.46	9.90	14.04	25.79	35.67	18.70
6b	3.65	9.91	14.37	26.05	35.12	18.15
6c	3.63	9.90	14.53	25.83	34.97	18.03
6d	3.62	9.84	14.44	25.94	35.21	18.42
6e	3.87	10.05	14.64	26.27	35.16	17.79
6f	3.77	10.04	14.48	26.55	35.65	18.30
6g	3.11	9.60	13.64	24.67	33.62	17.56
6h	3.39	9.69	13.79	25.5	34.75	18.42
6i	3.71	9.96	14.28	25.55	34.16	17.09
6j	3.78	9.93	13.89	25.82	34.78	17.74
6k	3.66	10.07	14.61	26.08	35.63	18.18
6l	3.65	9.99	13.71	25.39	34.93	17.70
6m	3.31	9.77	14.19	25.31	34.34	17.78
6n	3.42	9.86	14.44	25.81	35.12	18.28
6o	2.66	9.58	13.12	24.58	33.44	17.44
14a	3.43	8.60	12.83	25.39	32.89	19.78
14b	3.64	8.38	12.21	25.92	34.11	21.59
14c	3.44	8.64	12.51	25.01	32.70	19.48
14d	3.42	8.71	12.50	25.00	33.01	19.58
14e	3.65	8.57	12.58	25.31	34.47	21.40
14f	3.14	8.42	11.46	23.91	32.54	19.91
14g	3.29	8.46	12.20	24.48	33.19	20.44
14h	3.63	8.67	12.82	23.65	32.24	18.91
14i	3.38	8.58	12.48	23.11	31.29	18.21
14j	3.71	8.55	13.32	25.95	35.02	22.02
14k	3.33	8.55	12.40	24.71	33.30	20.30
14l	3.64	8.18	11.52	25.30	33.89	21.88
14m	3.26	8.53	12.14	25.74	33.92	20.98
14n	3.31	8.59	12.13	24.71	34.21	21.10
DFP	3.64	9.81	13.96	25.61	35.40	18.71
DFP <sup>b</sup>	3.61	9.78	15.03	27.42	37.35	20.74
DFP <sup>a</sup>	-	-	14.81	27.40	37.40	20.70

a: Compounds were measured in 0.1 M KCl. b: Data were from the corresponding reference and were tested in a 0.1 M KCl solution [41]. c: Compounds were tested in DMSO:0.1 M KCl = 1:1.5 (v/v) to address the solubility issue.

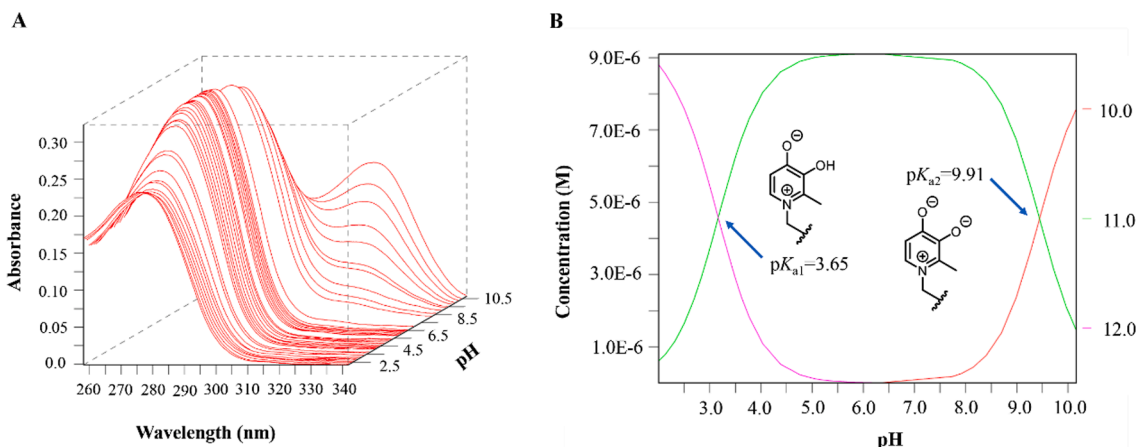


**Fig. 4.** The pH-dependent UV spectra of compounds **6b**. **A:** The pH-dependence of the titration spectrum of compound **6b**. **B:** The  $pK_a$  values of compound **6b** over the pH range of 1.3–11.0 in 0.1 M KCl at 25 °C.

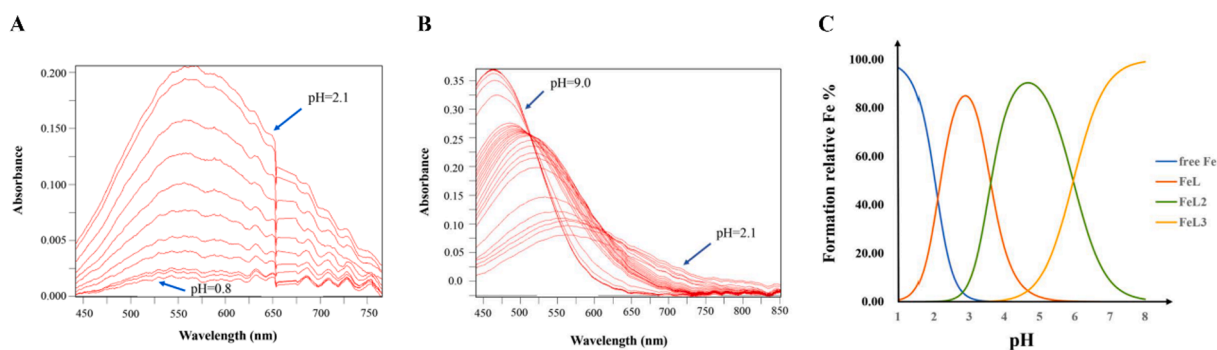


**Fig. 5.** The pH-dependent UV spectra of compound **6b**. **A:** The pH-dependence of the spectrum of compound **6b** in the presence of  $Fe^{3+}$  over the pH range 0.8 to 2.1 in 0.1 M KCl at 25 °C,  $[Fe^{3+}] = 1.0 \mu M$ ,  $[6b] = 1.1 \mu M$ . **B:** The pH-dependence of the spectrum of compound **6b** in the presence of  $Fe^{3+}$  over the pH range of 2.1 to 9.0 in 0.1 M KCl: DMSO = 3:2 (v/v) at 25 °C,  $[Fe^{3+}] = 1.0 \mu M$ ,  $[6b] = 5.0 \mu M$ . **C:** Speciation plot of  $Fe^{3+}/6b$  as measured by the percentage formation relative to  $[Fe^{3+}]_{total}$  as a function of pH. This plot was calculated from the affinity constants reported in Table 1, and the  $Fe^{3+}$  hydrolysis constants were as follows:  $\text{Log } \beta (Fe-H) = -2.563$ ,  $\text{Log } \beta (Fe-H_2) = -6.205$ ,  $\text{Log } \beta (Fe-H_3) = -15.100$ ,  $\text{Log } \beta (Fe_2-H_2) = -2.843$ ,  $\text{Log } \beta (Fe_3-H_4) = -6.059$ , and  $\text{Log } \beta (Fe-H_4) = -21.883$ .

**Table 2**  
hMAO-B inhibitory activities of the hybrid compounds.

Compound	Inhibitory rate $\pm$ SEM (%), 0.1 $\mu M$ <sup>a</sup>	Compound	Inhibitory rate $\pm$ SEM (%), 0.1 $\mu M$ <sup>a</sup>
6a	45 $\pm$ 2	14a	43.4 $\pm$ 0.1
6b	59 $\pm$ 2	14b	32 $\pm$ 2
6c	50 $\pm$ 4	14c	27.4 $\pm$ 0.1
6d	53 $\pm$ 2	14d	37 $\pm$ 2
6e	31.5 $\pm$ 0.4	14e	32.4 $\pm$ 0.9
6f	36.9 $\pm$ 0.4	14f	33 $\pm$ 1
6g	45 $\pm$ 4	14g	37.9 $\pm$ 0.5
6h	31 $\pm$ 3	14h	46.7 $\pm$ 0.7
6i	29.0 $\pm$ 0.1	14i	30 $\pm$ 3
6j	23.5 $\pm$ 0.5	14j	37 $\pm$ 1
6k	41 $\pm$ 2	14k	34 $\pm$ 2
6l	50 $\pm$ 2	14l	39 $\pm$ 1
6m	48 $\pm$ 2	14m	30 $\pm$ 2
6n	39 $\pm$ 1	14n	36 $\pm$ 2
6o	18.3 $\pm$ 0.6	pargyline	50 $\pm$ 3

a: Each inhibitory rate is the mean  $\pm$  SEM from two experiments.

compound **6b** displayed excellent selectivity for hMAO-B (hMAO-B  $IC_{50} = 0.083 \pm 0.001 \mu M$ , hMAO-A  $IC_{50} = 6.11 \pm 0.08 \mu M$ ; SI = 73.5). Therefore, summarizing the above assay results, compound **6b** acted as the most potent and selective MAO-B inhibitor.

**Table 3**  
 $IC_{50}$  values of the hybrid compounds.

Compound	$IC_{50} \pm$ SEM (hMAO-B) [ $\mu M$ ] <sup>a</sup>
6a	0.122 $\pm$ 0.002
6b	0.083 $\pm$ 0.001
6c	0.090 $\pm$ 0.003
6d	0.11 $\pm$ 0.01
6g	0.113 $\pm$ 0.003
6k	0.109 $\pm$ 0.002
6l	0.100 $\pm$ 0.007
6m	0.109 $\pm$ 0.002
14a	0.105 $\pm$ 0.003
14h	0.119 $\pm$ 0.005
pargyline	0.097 $\pm$ 0.004

a: Each  $IC_{50}$  value is the mean  $\pm$  SEM from two experiments.

**Table 4**  
Selectivity of compound **6b** and pargyline.

Compounds	$IC_{50} \pm$ SEM (hMAO-B) [ $\mu M$ ] <sup>a</sup>	$IC_{50} \pm$ SEM (hMAO-A) [ $\mu M$ ] <sup>a</sup>	Selectivity index <sup>b</sup>
6b	0.083 $\pm$ 0.001	6.11 $\pm$ 0.08	73.5
pargyline	0.097 $\pm$ 0.004	4.184 $\pm$ 0.005	40

a: Each  $IC_{50}$  value is the mean  $\pm$  SEM from two experiments. b: The selectivity index is defined as  $IC_{50}(hMAO-A)/IC_{50}(hMAO-B)$ .

## 2.4. Prediction of BBB permeability

Parallel artificial membrane permeability assay (PAMPA) was used to predict the BBB permeability of the screened compound. Seven commercial drugs were selected as references for the experiment. The comparison of the data in Table 5 outlined that the data obtained by our method had better reproducibility compared with the reported literatures [42,43], indicating that the final result had higher credibility. The  $Pe$  value of compound **6b** measured by this method was  $(3.21 \pm 0.08) \times 10^{-6}$  cm/s (CNS +/-), indicating that compound **6b** had the possibility of penetrating the BBB. In order to further confirm these results, we had selected three prediction platforms for verification.

The three different prediction platforms (ADMETlab [44], SwissADME [45], and admetSAR [46]) predicted several key physicochemical parameters and the ability of compound **6b** and the reference inhibitor to penetrate the BBB. As illustrated in Table 6, compound **6b** followed Lipinski's rule and could cross the BBB (BBB+). We also used the prediction results of the reference drug pargyline as verification.

Combining the results of the two experiments, it could be seen that compound **6b** was likely to pass through the BBB.

## 2.5. Mouse behavioral research

To further explore the activity of hybrid **6b** *in vivo*, the Morris water maze assay was selected as the anti-AD model. The mice were first intraperitoneally injected with pargyline (reference drug), **6b** or blank solution. Thirty minutes later, scopolamine (15 mg/kg) was intraperitoneally injected. Mice were treated with the test compound and reference drug for fifteen days. Learning and memory training was carried out days 11–14 (no movement track was recorded in the first two days) and the exploratory experiment was performed on the 15th day (for a total of five days). The analysis of the behavioral data on the 15th day and ballistic analysis are shown in Fig. 6 and Table 7.

From the perspective of the entries in Fig. 6A, the number of platform crossings of the model group mice reduced dramatically ( $2.0 \pm 0.5$  vs.  $5.7 \pm 0.9$ ,  $^{##}p < 0.01$ ). Compared with the model group, the mice treated with pargyline significantly improved cognitive impairment and increased the number of times they crossed the platform ( $3.8 \pm 0.5$  vs.  $2.0 \pm 0.5$ ,  $^{#}p < 0.05$ ). The **6b** group exhibited activity comparable to that of pargyline ( $4.2 \pm 0.7$  vs.  $2.0 \pm 0.5$ ,  $^{#}p < 0.05$ ). From the perspective of the latency to the target (Fig. 6B), compared with the blank group, scopolamine significantly prolonged the latency period of the mice to the target ( $41 \pm 6$  s vs.  $12 \pm 3$  s,  $^{###}p < 0.001$ ). Compared with the model group, the mice in the pargyline group required a shorter time to find the platform ( $14 \pm 3$  s vs.  $41 \pm 6$  s,  $^{**}p < 0.01$ ). The **6b** group also showed a great therapeutic effect ( $16 \pm 3$  s vs.  $41 \pm 6$  s,  $^{**}p < 0.01$ ).

**Table 5**

PAMPA-BBB results for seven commercial drugs and **6b**.

Compound	$Pe \pm SEM (\times 10^{-6})$ cm/s) <sup>a</sup>	$Pe (\times 10^{-6})$ cm/s)	PAMPA-BBB assay classification <sup>d</sup>
donepezil	$10 \pm 1$	$7.3 \pm 0.9$ <sup>b</sup>	CNS +
testosterone	$14 \pm 1$	$17$ <sup>c</sup>	CNS +
tacrine	$4.1 \pm 0.4$	$5.3 \pm 0.19$ <sup>b</sup>	CNS +
hydrocortisone	$2.00 \pm 0.04$	$1.9$ <sup>c</sup>	CNS +/-
piroxicam	$2.05 \pm 0.04$	$2.5$ <sup>c</sup>	CNS +/-
atenolol	$0.4 \pm 0.2$	$0.8$ <sup>c</sup>	CNS -
theophylline	$0.12 \pm 0.01$	$1.07 \pm 0.18$ <sup>b</sup>	CNS -
<b>6b</b>	$3.21 \pm 0.08$		CNS +/-

a: Data are the mean  $\pm$  SEM of eight independent experiments. b: Data were from Ref. [42] c: Data were from Ref. [43]. d: CNS (+) (high BBB permeation predicted);  $Pe (\times 10^{-6} \text{ cm s}^{-1}) > 4.0$ ; CNS (+/-) (BBB permeation uncertain);  $Pe (\times 10^{-6} \text{ cm s}^{-1})$  from 2.0 to 4.0; CNS (-) (low BBB permeation predicted);  $Pe (\times 10^{-6} \text{ cm s}^{-1}) < 2.0$ .

As shown in Fig. 6C, the mice treated with pargyline remarkably reduced the distance to the target compared with the model group ( $2.9 \pm 0.7$  m vs.  $8 \pm 1$  m,  $^{**}p < 0.01$ ). After injection of compound **6b**, the distance to the platform for the first time was reduced ( $3.1 \pm 0.5$  m vs.  $8 \pm 1$  m,  $^{**}p < 0.01$ ).

Based on the above results and comparing the trajectories of the mice in the different treatment groups (Fig. 6D), it was found that **6b** could significantly improve the cognitive impairment in mice induced by scopolamine. Similarly, this assay verified the results of the above prediction experiment of BBB permeability.

## 2.6. Discussion

As the results of iron-chelating determination shown the effects of modification at different positions of the pyridone ring are completely different. A series of compounds obtained by modifying the *N*-1 position of pyridone showed general iron-chelating activity, on the contrary, the activity of pyridone is better by retaining the *C*-1 methyl substitution of pyridone and modifying its *C*-6 position. According to relevant literatures, *N*-substituents have little effect on the affinity of iron [25], which was also confirmed by our experimental data ( $pFe^{3+} = 17.09$ – $18.70$  vs.  $pFe^{3+} = 18.71$ ). In comparison, the introduction of substituents at the *C*-6 position of pyridone could reduce the  $pK_a$  values and increase the  $pFe^{3+}$  values consequently which was consistent with the negative inductive effect of the substituents at the *C*-6 position.

Similarly, the MAO-B inhibitory assay results, we conducted the same analysis: Combining analysis of Table 2 and Table 3, when a small hindered substituent (alkynyl or methyl) was introduced onto the *N*-H of the *N*-propargylamine moiety, the enzyme inhibitory activity decreased significantly compared with the introduction of large hindered groups (phenyl), which indicated that a large hindering group was beneficial to occupy the active cavity of MAO-B and showed potent activity; additionally, the presence of electron-withdrawing group (especially F) on the benzene ring was also beneficial to increase the activity.

In the BBB permeability prediction experiments, the PAMPA-BBB simulation results were different from the results obtained from the three prediction platforms. We speculated that there was a certain error in the PAMPA assay results. It could be seen from the numerical of commercial drugs that the data measured by our method was relatively decrease, compared with the values reported in the literature [42,43]. Therefore, we speculated compound **6b** was likely to cross the BBB.

## 3. Conclusions

Based on the MTDL drug design and pharmacophore fusion strategy,

**Table 6**  
Predicted results from the three different prediction platforms.

Platform	Compound	MW	HBDs	HBAs	Log P	TPSA	BBB ( $\pm$ )
ADMETlab <sup>a</sup>	<b>6b</b>	314.36	1	4	2.137	45.47	+
	pargyline	159.23	0	1	1.752	3.24	+
SwissADME <sup>b</sup>	<b>6b</b>	314.35	1	4	2.63	45.47	+
	pargyline	159.23	0	1	2.50	3.24	+
admetSAR 2.0 <sup>c</sup>	<b>6b</b>	314.36	1	4	2.14	/	+
	pargyline	159.23	0	1	1.75	/	+
	CNS drug	$\leq 450$	$\leq 5$	$\leq 10$	$\leq 5$	$\leq 90$	

a: The ADMETlab web platform is designed based on the Django framework in Python, and is freely accessible at <http://admet.scbdd.com/>. b: SwissADME is freely accessible at <http://www.swissadme.ch>. c: admetSAR 2.0 is freely accessible at <http://www.admetexp.org>. MW: molecular weight; HBDs: H-bond donors; HBAs: H-bond acceptors; Log P: log octanol/water partition coefficient; TPSA: topological polar surface area; BBB ( $\pm$ ): BBB permeability.

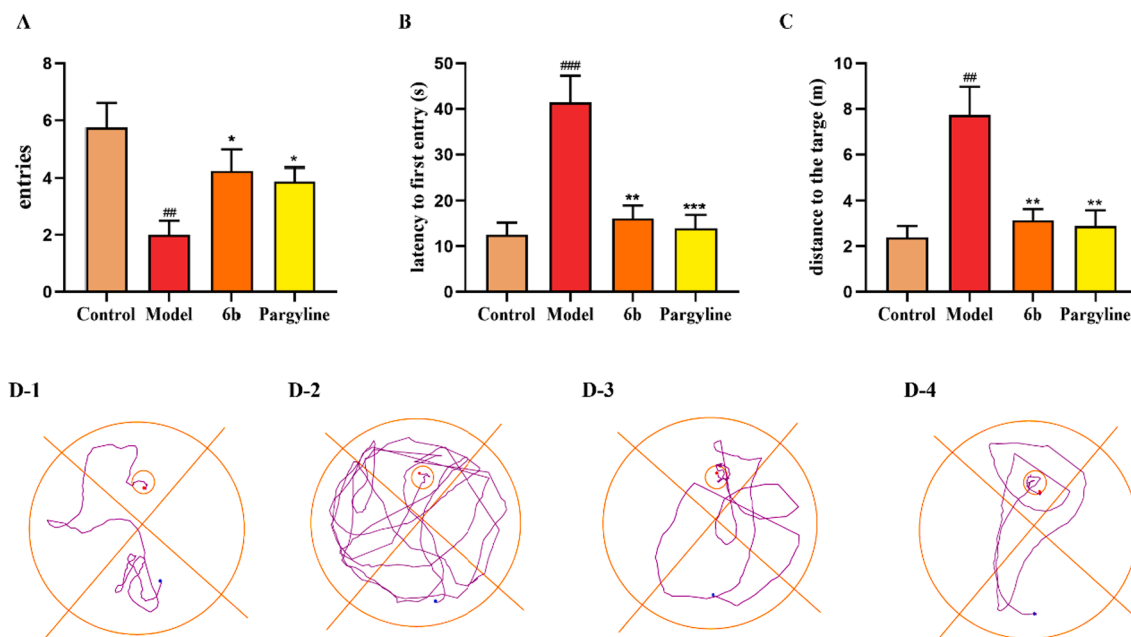


**Fig. 6.** Pargyline (15 mg/kg) and compound **6b** (15 mg/kg) were evaluated for scopolamine-induced (15 mg/kg) memory impairment in ICR mice in the Morris water maze. The mouse trajectories of the mice are shown as the control (D-1), model (D-2), **6b** (D-3), and pargyline (D-4) groups.

**Table 7**

Effects of compound **6b** (15 mg/kg) on scopolamine-induced memory impairment in ICR mice evaluated by the Morris water maze test. Pargyline (15 mg/kg) was used as the reference control. Data are presented as the mean  $\pm$  SEM (n = 8; # p < 0.05, ## p < 0.01, ### p < 0.001, control group vs. scopolamine model group; \*p < 0.05, \*\*p < 0.01, \*\*\*p < 0.001, pargyline group or **6b** vs. scopolamine model group).

Group	Entries	Latency to the first entry	Distance to the target
Control	5.7 $\pm$ 0.9	12 $\pm$ 3	2.4 $\pm$ 0.5
Model	2.0 $\pm$ 0.5##	41 $\pm$ 6###	8 $\pm$ 1##
<b>6b</b>	4.2 $\pm$ 0.7*	16 $\pm$ 3**	3.1 $\pm$ 0.5**
Pargyline	3.8 $\pm$ 0.5*	14 $\pm$ 3**	2.9 $\pm$ 0.7**

N-propargylamine-hydroxypyridinone hybrids were designed as potential lead compounds for AD therapy. The hybrids displayed promising iron-chelating activity and potent MAO-B inhibitory activity in the *in vitro* tests. In *in vitro* experiments, the hybrid showed promising iron chelation activity and effective MAO-B inhibitory activity. Compounds **14a-n** ( $pFe^{3+} = 18.21$ – $22.02$ ) inherited the iron-chelating ability of DFP ( $pFe^{3+} = 18.71$ ), indicating that the structural core of the designed has reached our design expectations. Moreover, the hMAO-B inhibitory ability of compounds **6b** ( $IC_{50} = 0.083 \pm 0.001 \mu M$ ) and **6c** ( $IC_{50} = 0.090 \pm 0.003 \mu M$ ) were the most potent compared to pargyline ( $IC_{50} = 0.097 \pm 0.004 \mu M$ ). Compound **6b** also showed excellent selectivity for

hMAO-B ( $hMAO-A IC_{50} = 6.11 \pm 0.08 \mu M$ ; SI = 73.5). More importantly, the BBB permeability of **6b** was predicted on multiple platforms, and all of the results displayed favorable BBB permeability. In the mouse Morris water maze model, **6b** significantly ameliorated the cognitive dysfunction induced by scopolamine through behavioral evaluation. Overall, compound **6b** is a multitarget hybrid with potential anti-AD activity.

## 4. Experimental section

### 4.1. General information

A capillary melting point instrument (B-540, Büchi, Switzerland) was used to determine the melting point of the compounds. The NMR spectra of  $^1H$  at 400 Hz or 600 Hz and  $^{13}C$  at 100 Hz with  $CDCl_3$  or  $DMSO-d_6$  as the deuterated solvent were recorded on a Bruker instrument. Chemical shifts ( $\delta$ ) are reported in parts per million (ppm) relative to residual solvent as an internal reference. HRMS was recorded on a Bruker instrument (MICR OTOF-Q II). The purity of the hybrids was determined by high-performance liquid chromatography (HPLC) and confirmed to be over 96%. The instrument (Agilent) consisted of pumps (G1311A, Waldbronn, Germany), C18 column (4.6 mm  $\times$  150 mm, 5  $\mu m$ ; Atlantis, Ireland), and UV detector (G1315D, Agilent, America). Compounds **6a-o**: 40% acetonitrile/60% deionized water (0.15% HCOOH) with a flow rate of 0.5 mL/min; compounds **14a-n**: 60% methanol/40% deionized water (0.15%  $Et_3N$ ) with a flow rate of 0.5 mL/min.

#### 4.2. Preparation method of intermediate 4

At room temperature,  $K_2CO_3$  (1.5 mmol) was added to a solution of intermediate **3** (1.0 mmol) in DMF (10 mL). After ten minutes, a solution of 3-bromopropyne (0.8 mmol) in DMF (8 mL) was added to the above solution. The resulting mixture was stirred for 6 h. Finally, the solvent was removed, and the obtained crude material was separated and purified by column chromatography (DCM:MeOH = 25:1) to obtain intermediate **4** as a yellow oil.

##### 4.2.1. 3-(Benzyloxy)-2-methyl-1-(2-(prop-2-yn-1-ylamino)ethyl)pyridin-4(1H)-one (**4**)

Yield: 40%, yellow oil.  $^1H$  NMR (400 MHz,  $CDCl_3$ )  $\delta$  7.42 (dt,  $J$  = 7.5, 1.8 Hz, 2H), 7.37–7.29 (m, 3H), 7.28 (d,  $J$  = 2.4 Hz, 2H), 6.42 (d,  $J$  = 7.6 Hz, 1H), 5.22 (s, 2H), 3.90 (t,  $J$  = 6.4 Hz, 2H), 3.40 (t,  $J$  = 2.4 Hz, 2H), 2.95 (t,  $J$  = 6.4 Hz, 2H), 2.26 (t,  $J$  = 2.4 Hz, 1H), 2.13 (s, 3H).

#### 4.3. Preparation method of intermediates 5a-o

A mixture of the corresponding substituted benzyl bromides, methyl iodide or 3-bromopropyne (1.5 mmol), intermediate **4** (1.0 mmol) and KOH (1.5 mmol) in THF (20 mL) reacted for 20 h. The solvent was concentrated, and then the crude material was purified by column chromatography (DCM/MeOH = 30:1) to obtain **5a-o** as yellow oils.

##### 4.3.1. 1-(2-(Benzyl(prop-2-yn-1-yl)amino)ethyl)-3-(benzyloxy)-2-methylpyridin-4(1H)-one (**5a**)

Yield: 65%, yellow oil.  $^1H$  NMR (400 MHz,  $CDCl_3$ )  $\delta$  7.43–7.36 (m, 2H), 7.31 (d,  $J$  = 5.8 Hz, 2H), 7.28–7.24 (m, 4H), 7.24–7.18 (m, 2H), 7.15 (d,  $J$  = 7.5 Hz, 1H), 6.40 (d,  $J$  = 7.5 Hz, 1H), 5.21 (s, 2H), 3.76 (t,  $J$  = 6.5 Hz, 2H), 3.62 (s, 2H), 3.33 (d,  $J$  = 2.3 Hz, 2H), 2.74 (t,  $J$  = 6.5 Hz, 2H), 2.29 (t,  $J$  = 2.3 Hz, 1H), 2.00 (s, 3H).

##### 4.3.2. 3-(Benzyloxy)-1-(2-((2-fluorobenzyl)(prop-2-yn-1-yl)amino)ethyl)-2-methylpyridin-4(1H)-one (**5b**)

Yield: 70%, yellow oil.  $^1H$  NMR (400 MHz,  $CDCl_3$ )  $\delta$  7.43–7.35 (m, 2H), 7.34–7.27 (m, 4H), 7.25–7.17 (m, 2H), 7.11–6.99 (m, 2H), 6.45 (d,  $J$  = 7.5 Hz, 1H), 5.21 (s, 2H), 3.81 (t,  $J$  = 6.5 Hz, 2H), 3.69 (s, 2H), 3.32 (d,  $J$  = 2.3 Hz, 2H), 2.78 (t,  $J$  = 6.5 Hz, 2H), 2.28 (t,  $J$  = 2.3 Hz, 1H), 2.04 (s, 3H).

##### 4.3.3. 3-(Benzyloxy)-1-(2-((3-fluorobenzyl)(prop-2-yn-1-yl)amino)ethyl)-2-methylpyridin-4(1H)-one (**5c**)

Yield: 66%, yellow oil.  $^1H$  NMR (400 MHz,  $CDCl_3$ )  $\delta$  7.41 (dd,  $J$  = 7.4, 2.2 Hz, 2H), 7.35–7.29 (m, 3H), 7.26 (d,  $J$  = 8.3 Hz, 1H), 7.17 (d,  $J$  = 7.5 Hz, 1H), 7.04–6.91 (m, 3H), 6.43 (d,  $J$  = 7.5 Hz, 1H), 5.22 (s, 2H), 3.80 (t,  $J$  = 6.5 Hz, 2H), 3.63 (s, 2H), 3.33 (d,  $J$  = 2.3 Hz, 2H), 2.76 (t,  $J$  = 6.5 Hz, 2H), 2.30 (t,  $J$  = 2.3 Hz, 1H), 2.04 (s, 3H).

##### 4.3.4. 3-(Benzyloxy)-1-(2-((4-fluorobenzyl)(prop-2-yn-1-yl)amino)ethyl)-2-methylpyridin-4(1H)-one (**5d**)

Yield: 71%, yellow oil.  $^1H$  NMR (400 MHz,  $CDCl_3$ )  $\delta$  7.50–7.40 (m, 3H), 7.40–7.31 (m, 5H), 7.24–7.16 (m, 2H), 6.42 (d,  $J$  = 7.5 Hz, 1H), 5.23 (s, 2H), 3.81 (t,  $J$  = 6.6 Hz, 2H), 3.61 (s, 2H), 3.33 (d,  $J$  = 2.3 Hz, 2H), 2.77 (t,  $J$  = 6.5 Hz, 2H), 2.33 (d,  $J$  = 2.3 Hz, 1H), 2.05 (s, 3H).

##### 4.3.5. 3-(Benzyloxy)-1-(2-((2-chlorobenzyl)(prop-2-yn-1-yl)amino)ethyl)-2-methylpyridin-4(1H)-one (**5e**)

Yield: 60%, yellow oil.  $^1H$  NMR (400 MHz,  $CDCl_3$ )  $\delta$  7.84 (dd,  $J$  = 7.9, 1.4 Hz, 1H), 7.55 (td,  $J$  = 7.5, 1.4 Hz, 1H), 7.46 (td,  $J$  = 7.8, 1.5 Hz, 1H), 7.42 (d,  $J$  = 2.5 Hz, 2H), 7.40 (d,  $J$  = 1.9 Hz, 1H), 7.36–7.29 (m, 3H), 7.14 (d,  $J$  = 7.5 Hz, 1H), 6.40 (d,  $J$  = 7.5 Hz, 1H), 5.22 (s, 2H), 4.00 (s, 2H), 3.78 (t,  $J$  = 6.5 Hz, 2H), 3.22 (d,  $J$  = 2.3 Hz, 2H), 2.76 (t,  $J$  = 6.5 Hz, 2H), 2.31 (t,  $J$  = 2.3 Hz, 1H), 2.03 (s, 3H).

##### 4.3.6. 3-(Benzyloxy)-1-(2-((3-chlorobenzyl)(prop-2-yn-1-yl)amino)ethyl)-2-methylpyridin-4(1H)-one (**5f**)

Yield: 65%, yellow oil.  $^1H$  NMR (400 MHz,  $CDCl_3$ )  $\delta$  7.38 (dd,  $J$  = 7.5, 2.1 Hz, 2H), 7.32–7.27 (m, 3H), 7.23 (d,  $J$  = 2.6 Hz, 3H), 7.16 (d,  $J$  = 7.5 Hz, 1H), 7.10–7.04 (m, 1H), 6.41 (d,  $J$  = 7.5 Hz, 1H), 5.20 (s, 2H), 3.78 (t,  $J$  = 6.5 Hz, 2H), 3.59 (s, 2H), 3.31 (d,  $J$  = 2.4 Hz, 2H), 2.73 (t,  $J$  = 6.5 Hz, 2H), 2.28 (t,  $J$  = 2.3 Hz, 1H), 2.02 (s, 3H).

##### 4.3.7. 3-(Benzyloxy)-1-(2-((4-chlorobenzyl)(prop-2-yn-1-yl)amino)ethyl)-2-methylpyridin-4(1H)-one (**5g**)

Yield: 68%, yellow oil.  $^1H$  NMR (400 MHz,  $CDCl_3$ )  $\delta$  7.39 (m, 2H), 7.34–7.25 (m, 4H), 7.18 (d,  $J$  = 7.4 Hz, 1H), 7.15–7.11 (m, 3H), 6.46 (d,  $J$  = 7.4 Hz, 1H), 5.21 (s, 2H), 3.80 (t,  $J$  = 6.5 Hz, 2H), 3.58 (s, 2H), 3.30 (d,  $J$  = 2.4 Hz, 2H), 2.74 (t,  $J$  = 6.5 Hz, 2H), 2.28 (t,  $J$  = 2.3 Hz, 1H), 2.02 (s, 3H).

##### 4.3.8. 3-(Benzyloxy)-1-(2-(di(prop-2-yn-1-yl)amino)ethyl)-2-methylpyridin-4(1H)-one (**5h**)

Yield: 59%, yellow oil.  $^1H$  NMR (400 MHz,  $CDCl_3$ )  $\delta$  7.45–7.40 (m, 2H), 7.36 (d,  $J$  = 8.6 Hz, 1H), 7.33 (d,  $J$  = 2.0 Hz, 2H), 7.31 (d,  $J$  = 5.4 Hz, 1H), 6.51 (d,  $J$  = 7.4 Hz, 1H), 5.26 (s, 2H), 3.90 (t,  $J$  = 6.7 Hz, 2H), 3.38 (d,  $J$  = 2.4 Hz, 4H), 2.81 (t,  $J$  = 6.7 Hz, 2H), 2.27 (t,  $J$  = 2.4 Hz, 2H), 2.15 (s, 3H).

##### 4.3.9. 3-(Benzyloxy)-2-methyl-1-(2-(prop-2-yn-1-yl(3-(trifluoromethyl)benzyl)amino)ethyl)pyridin-4(1H)-one (**5i**)

Yield: 70%, yellow oil.  $^1H$  NMR (400 MHz,  $CDCl_3$ )  $\delta$  7.58–7.52 (m, 2H), 7.45 (t,  $J$  = 7.6 Hz, 1H), 7.43–7.37 (m, 3H), 7.35–7.29 (m, 3H), 7.21 (d,  $J$  = 7.5 Hz, 1H), 6.48 (d,  $J$  = 7.4 Hz, 1H), 5.23 (s, 2H), 3.84 (t,  $J$  = 6.6 Hz, 2H), 3.70 (s, 2H), 3.35 (d,  $J$  = 2.4 Hz, 2H), 2.78 (t,  $J$  = 6.6 Hz, 2H), 2.33 (t,  $J$  = 2.4 Hz, 1H), 2.04 (s, 3H).

##### 4.3.10. 3-(Benzyloxy)-2-methyl-1-(2-(prop-2-yn-1-yl(4-(trifluoromethyl)benzyl)amino)ethyl)pyridin-4(1H)-one (**5j**)

Yield: 64%, yellow oil.  $^1H$  NMR (400 MHz,  $CDCl_3$ )  $\delta$  7.57 (d,  $J$  = 7.9 Hz, 2H), 7.42–7.36 (m, 2H), 7.36–7.32 (m, 2H), 7.29 (m, 3H), 7.21 (d,  $J$  = 7.5 Hz, 1H), 6.49 (d,  $J$  = 7.5 Hz, 1H), 5.22 (s, 2H), 3.83 (t,  $J$  = 6.5 Hz, 2H), 3.67 (s, 2H), 3.30 (d,  $J$  = 2.3 Hz, 2H), 2.77 (t,  $J$  = 6.5 Hz, 2H), 2.29 (t,  $J$  = 2.3 Hz, 1H), 2.03 (s, 3H).

##### 4.3.11. 3-(Benzyloxy)-1-(2-((2,5-difluorobenzyl)(prop-2-yn-1-yl)amino)ethyl)-2-methylpyridin-4(1H)-one (**5k**)

Yield: 66%, yellow oil.  $^1H$  NMR (400 MHz,  $CDCl_3$ )  $\delta$  7.41 (d,  $J$  = 2.3 Hz, 1H), 7.39 (q,  $J$  = 2.5, 2.0 Hz, 1H), 7.35–7.25 (m, 3H), 7.19 (d,  $J$  = 7.5 Hz, 1H), 7.05–6.88 (m, 3H), 6.42 (d,  $J$  = 7.5 Hz, 1H), 5.21 (s, 2H), 3.82 (t,  $J$  = 6.5 Hz, 2H), 3.66 (d,  $J$  = 1.2 Hz, 2H), 3.31 (d,  $J$  = 2.4 Hz, 2H), 2.78 (t,  $J$  = 6.5 Hz, 2H), 2.29 (t,  $J$  = 2.4 Hz, 1H), 2.06 (s, 3H).

##### 4.3.12. 3-(Benzyloxy)-1-(2-((3,5-difluorobenzyl)(prop-2-yn-1-yl)amino)ethyl)-2-methylpyridin-4(1H)-one (**5l**)

Yield: 62%, yellow oil.  $^1H$  NMR (400 MHz,  $CDCl_3$ )  $\delta$  7.48–7.37 (m, 2H), 7.32 (d,  $J$  = 5.7 Hz, 1H), 7.20 (d,  $J$  = 7.5 Hz, 1H), 6.79 (d,  $J$  = 6.3 Hz, 4H), 6.72 (td,  $J$  = 7.6, 6.4, 4.4 Hz, 1H), 6.41 (d,  $J$  = 7.5 Hz, 1H), 5.22 (s, 2H), 3.84 (t,  $J$  = 6.7 Hz, 2H), 3.62 (s, 2H), 3.32 (d,  $J$  = 2.4 Hz, 2H), 2.77 (t,  $J$  = 6.7 Hz, 2H), 2.32 (d,  $J$  = 2.4 Hz, 1H), 2.07 (s, 3H).

##### 4.3.13. 3-(Benzyloxy)-2-methyl-1-(2-((3-methylbenzyl)(prop-2-yn-1-yl)amino)ethyl)pyridin-4(1H)-one (**5m**)

Yield: 69%, yellow oil.  $^1H$  NMR (400 MHz,  $CDCl_3$ )  $\delta$  7.41 (dt,  $J$  = 6.6, 2.6 Hz, 2H), 7.36–7.32 (m, 1H), 7.30 (dd,  $J$  = 5.5, 1.7 Hz, 2H), 7.26–7.17 (m, 2H), 7.10 (d,  $J$  = 7.6 Hz, 1H), 7.07–7.00 (m, 2H), 6.48 (d,  $J$  = 7.4 Hz, 1H), 5.23 (s, 2H), 3.80 (t,  $J$  = 6.6 Hz, 2H), 3.61 (s, 2H), 3.35 (d,  $J$  = 2.4 Hz, 2H), 2.77 (t,  $J$  = 6.6 Hz, 2H), 2.35 (s, 3H), 2.30 (t,  $J$  = 2.4 Hz, 1H), 2.03 (s, 3H).

#### 4.3.14. 3-(Benzyloxy)-2-methyl-1-(2-((4-methylbenzyl)(prop-2-yn-1-yl)amino)ethyl)pyridin-4(1H)-one (5n)

Yield: 61%, yellow oil.  $^1\text{H}$  NMR (400 MHz,  $\text{CDCl}_3$ )  $\delta$  7.46–7.39 (m, 2H), 7.37–7.28 (m, 3H), 7.19 (d,  $J = 7.5$  Hz, 1H), 7.15–7.09 (m, 4H), 6.49 (d,  $J = 7.4$  Hz, 1H), 5.23 (s, 2H), 3.79 (t,  $J = 6.5$  Hz, 2H), 3.60 (s, 2H), 3.34 (d,  $J = 2.4$  Hz, 2H), 2.76 (t,  $J = 6.5$  Hz, 2H), 2.35 (s, 3H), 2.29 (t,  $J = 2.4$  Hz, 1H), 2.02 (s, 3H).

#### 4.3.15. 3-(Benzyloxy)-2-methyl-1-(2-(methyl(prop-2-yn-1-yl)amino)ethyl)pyridin-4(1H)-one (5o)

Yield: 55%, yellow oil.  $^1\text{H}$  NMR (400 MHz,  $\text{CDCl}_3$ )  $\delta$  7.45–7.40 (m, 2H), 7.39–7.33 (m, 1H), 7.33 (q,  $J = 1.7$  Hz, 2H), 7.26 (s, 1H), 6.48 (d,  $J = 7.4$  Hz, 1H), 5.24 (s, 2H), 3.85 (t,  $J = 6.7$  Hz, 2H), 3.31 (d,  $J = 2.4$  Hz, 2H), 2.66 (t,  $J = 6.7$  Hz, 2H), 2.32 (s, 3H), 2.26 (t,  $J = 2.4$  Hz, 1H), 2.13 (s, 3H).

### 4.4. Preparation method of compounds 6a-o

Intermediates **5a-o** (1 mmol) were completely dissolved in anhydrous DCM (10 mL), and then 3 mL of  $\text{BCl}_3$  solution (1 mmol/L in DCM) was added at  $-30$  °C. The reaction was carried out under nitrogen protection. After the addition, the reaction was continuously stirred for 2 h, quenched with methanol (15 mL), warmed to room temperature and stirred for 12 h. The solvent was concentrated, and the obtained crude material was purified by recrystallization (methanol/ether) to obtain **6a-o** as white solids.

#### 4.4.1. 1-(2-(Benzyl(prop-2-yn-1-yl)amino)ethyl)-3-hydroxy-2-methylpyridin-4(1H)-one (6a)

Yield: 75%, white solid, m.p. 174.3–176.1 °C,  $^1\text{H}$  NMR (400 MHz,  $\text{DMSO}-d_6$ )  $\delta$  10.51 (br, 1H), 8.22 (d,  $J = 7.0$  Hz, 1H), 7.39 (d,  $J = 6.9$  Hz, 1H), 7.32 (s, 5H), 4.69 (br, 2H), 4.01 (s, 2H), 3.75 (s, 2H), 3.61 (s, 1H), 3.28 (br, 2H), 2.41 (s, 3H).  $^{13}\text{C}$  NMR (100 MHz,  $\text{DMSO}-d_6$ )  $\delta$  159.4, 150.2, 143.4, 142.4, 139.2, 136.6, 130.8, 129.1, 111.2, 80.7, 74.7, 57.2, 51.7, 50.8, 42.0, 13.2. HRMS (ESI):  $m/z$  calcd for  $\text{C}_{18}\text{H}_{21}\text{N}_2\text{O}_2$  [ $\text{M} + \text{H}$ ] $^+$ : 297.1598 found 297.1596. HPLC purity: 100%.

#### 4.4.2. 1-(2-((2-Fluorobenzyl)(prop-2-yn-1-yl)amino)ethyl)-3-hydroxy-2-methylpyridin-4(1H)-one (6b)

Yield: 72%, white solid, m.p. 188.2–190.2 °C,  $^1\text{H}$  NMR (400 MHz,  $\text{DMSO}-d_6$ )  $\delta$  10.41 (br, 1H), 8.08 (d,  $J = 7.0$  Hz, 1H), 7.29 (m, 2H), 7.18–6.99 (m, 3H), 4.49 (d,  $J = 5.6$  Hz, 2H), 3.77 (s, 2H), 3.62 (s, 2H), 3.37 (s, 1H), 2.95 (br, 2H), 2.36 (s, 3H).  $^{13}\text{C}$  NMR (100 MHz,  $\text{DMSO}-d_6$ )  $\delta$  161.2 (d,  $^1J_{\text{C-F}} = 244.8$  Hz), 159.0, 143.2, 142.1, 139.7, 139.1, 132.2, 130.6 (d,  $^3J_{\text{C-F}} = 7.5$  Hz), 124.7 (d,  $^4J_{\text{C-F}} = 3.1$  Hz), 115.8 (d,  $^2J_{\text{C-F}} = 21.4$  Hz), 110.8, 78.4, 77.6, 53.1, 51.0, 50.7, 42.4, 13.0. HRMS (ESI):  $m/z$  calcd for  $\text{C}_{18}\text{H}_{20}\text{FN}_2\text{O}_2$  [ $\text{M} + \text{H}$ ] $^+$ : 315.1503 found 315.1484. HPLC purity: 99.26%.

#### 4.4.3. 1-(2-((3-Fluorobenzyl)(prop-2-yn-1-yl)amino)ethyl)-3-hydroxy-2-methylpyridin-4(1H)-one (6c)

Yield: 70%, white solid, m.p. 151.6–153.1 °C,  $^1\text{H}$  NMR (400 MHz,  $\text{DMSO}-d_6$ )  $\delta$  10.51 (br, 1H), 8.19 (d,  $J = 6.8$  Hz, 1H), 7.36 (s, 1H), 7.31 (t,  $J = 7.1$  Hz, 1H), 7.19–6.98 (m, 3H), 4.62 (br, 2H), 3.92 (s, 2H), 3.72 (s, 2H), 3.52 (s, 1H), 3.09 (br, 2H), 2.40 (s, 3H).  $^{13}\text{C}$  NMR (100 MHz,  $\text{DMSO}-d_6$ )  $\delta$  162.4 (d,  $^1J_{\text{C-F}} = 242.6$  Hz), 159.2, 143.4, 142.3, 139.2, 130.9 (d,  $^3J_{\text{C-F}} = 8.1$  Hz), 129.0, 126.3, 116.9 (d,  $^2J_{\text{C-F}} = 20.5$  Hz), 115.7 (d,  $^2J_{\text{C-F}} = 20.9$  Hz), 111.0, 79.7, 76.4, 56.9, 52.3, 51.0, 42.2, 13.2. HRMS (ESI):  $m/z$  calcd for  $\text{C}_{18}\text{H}_{20}\text{FN}_2\text{O}_2$  [ $\text{M} + \text{H}$ ] $^+$ : 315.1503 found 315.1496. HPLC purity: 98.88%.

#### 4.4.4. 1-(2-((4-Fluorobenzyl)(prop-2-yn-1-yl)amino)ethyl)-3-hydroxy-2-methylpyridin-4(1H)-one (6d)

Yield: 80%, white solid, m.p. 157.6–159.4 °C,  $^1\text{H}$  NMR (400 MHz,  $\text{DMSO}-d_6$ )  $\delta$  10.55 (br, 1H), 8.22 (d,  $J = 7.0$  Hz, 1H), 7.37 (t,  $J = 7.8$  Hz, 3H), 7.13 (t,  $J = 8.6$  Hz, 2H), 4.68 (br, 2H), 3.99 (s, 2H), 3.74 (s, 2H),

3.59 (s, 1H), 3.22 (br, 2H), 2.43 (s, 3H).  $^{13}\text{C}$  NMR (100 MHz,  $\text{DMSO}-d_6$ )  $\delta$  162.7 (d,  $^1J_{\text{C-F}} = 243.7$  Hz), 161.5, 159.3, 143.4, 142.4, 139.2, 133.0, 133.0, 115.9 (d,  $^2J_{\text{C-F}} = 21.3$  Hz), 111.1, 80.6, 75.4, 56.3, 51.7, 50.8, 41.9, 13.3. HRMS (ESI):  $m/z$  calcd for  $\text{C}_{18}\text{H}_{20}\text{FN}_2\text{O}_2$  [ $\text{M} + \text{H}$ ] $^+$ : 315.1503 found 315.1503. HPLC purity: 99.80%.

#### 4.4.5. 1-(2-((2-Chlorobenzyl)(prop-2-yn-1-yl)amino)ethyl)-3-hydroxy-2-methylpyridin-4(1H)-one (6e)

Yield: 65%, white solid, m.p. 189.7–191.3 °C,  $^1\text{H}$  NMR (400 MHz,  $\text{DMSO}-d_6$ )  $\delta$  10.38 (br, 1H), 8.01 (d,  $J = 7.0$  Hz, 1H), 7.31–6.99 (m, 5H), 4.42 (t,  $J = 5.6$  Hz, 2H), 3.68 (s, 2H), 3.60 (d,  $J = 2.4$  Hz, 2H), 3.32 (d,  $J = 2.2$  Hz, 1H), 2.88 (d,  $J = 5.6$  Hz, 2H), 2.33 (s, 3H).  $^{13}\text{C}$  NMR (100 MHz,  $\text{DMSO}-d_6$ )  $\delta$  158.9, 143.2, 142.0, 139.1, 134.5, 134.2, 131.7, 129.9, 129.0, 127.4, 110.8, 78.2, 77.7, 55.1, 53.4, 51.1, 42.5, 13.0. HRMS (ESI):  $m/z$  calcd for  $\text{C}_{18}\text{H}_{20}\text{ClN}_2\text{O}_2$  [ $\text{M} + \text{H}$ ] $^+$ : 331.1208 found 331.1192. HPLC purity: 96.80%.

#### 4.4.6. 1-(2-((3-Chlorobenzyl)(prop-2-yn-1-yl)amino)ethyl)-3-hydroxy-2-methylpyridin-4(1H)-one (6f)

Yield: 78%, white solid, m.p. 209.2–210.8 °C,  $^1\text{H}$  NMR (400 MHz,  $\text{DMSO}-d_6$ )  $\delta$  10.50 (br, 1H), 8.15 (d,  $J = 7.0$  Hz, 1H), 7.29 (dt,  $J = 22.0$ , 7.3 Hz, 3H), 7.20–7.07 (m, 2H), 4.55 (d,  $J = 5.6$  Hz, 2H), 3.80 (s, 2H), 3.67 (s, 2H), 3.45 (s, 1H), 2.99 (br, 2H), 2.39 (s, 3H).  $^{13}\text{C}$  NMR (100 MHz,  $\text{DMSO}-d_6$ )  $\delta$  159.2, 143.4, 142.1, 139.2, 133.6, 130.6, 129.6, 129.1, 128.5, 128.4, 110.9, 78.8, 77.3, 57.0, 52.8, 51.1, 42.2, 13.1. HRMS (ESI):  $m/z$  calcd for  $\text{C}_{18}\text{H}_{20}\text{ClN}_2\text{O}_2$  [ $\text{M} + \text{H}$ ] $^+$ : 331.1208 found 331.1197. HPLC purity: 100%.

#### 4.4.7. 1-(2-((4-Chlorobenzyl)(prop-2-yn-1-yl)amino)ethyl)-3-hydroxy-2-methylpyridin-4(1H)-one (6g)

Yield: 69%, white solid, m.p. 161.5–163.2 °C,  $^1\text{H}$  NMR (400 MHz,  $\text{DMSO}-d_6$ )  $\delta$  10.49 (br, 1H), 8.14 (d,  $J = 7.0$  Hz, 1H), 7.31 (t,  $J = 7.5$  Hz, 3H), 7.18 (s, 2H), 4.55 (br, 2H), 3.78 (s, 2H), 3.60 (s, 2H), 3.41 (s, 1H), 2.98 (br, 2H), 2.40 (s, 3H).  $^{13}\text{C}$  NMR (100 MHz,  $\text{DMSO}-d_6$ )  $\delta$  159.4, 143.4, 142.4, 139.2, 135.4, 133.8, 132.5, 129.0, 111.2, 80.2, 75.8, 56.5, 52.0, 51.1, 42.0, 13.3. HRMS (ESI):  $m/z$  calcd for  $\text{C}_{18}\text{H}_{20}\text{ClN}_2\text{O}_2$  [ $\text{M} + \text{H}$ ] $^+$ : 331.1208 found 331.1222. HPLC purity: 100%.

#### 4.4.8. 1-(2-(Di(prop-2-yn-1-yl)amino)ethyl)-3-hydroxy-2-methylpyridin-4(1H)-one (6h)

Yield: 85%, white solid, m.p. 196.4–198.2 °C,  $^1\text{H}$  NMR (400 MHz,  $\text{DMSO}-d_6$ )  $\delta$  10.49 (s, 1H), 8.18 (d,  $J = 7.0$  Hz, 1H), 7.36 (d,  $J = 6.9$  Hz, 1H), 4.52 (t,  $J = 6.1$  Hz, 2H), 3.54 (d,  $J = 2.3$  Hz, 4H), 3.27 (d,  $J = 2.3$  Hz, 2H), 2.97 (t,  $J = 6.1$  Hz, 2H), 2.56 (s, 3H).  $^{13}\text{C}$  NMR (100 MHz,  $\text{DMSO}-d_6$ )  $\delta$  159.2, 143.3, 142.5, 139.3, 110.9, 78.0, 77.7, 52.9, 51.5, 42.5, 13.3. HRMS (ESI):  $m/z$  calcd for  $\text{C}_{14}\text{H}_{17}\text{N}_2\text{O}_2$  [ $\text{M} + \text{H}$ ] $^+$ : 245.1285 found 245.1280. HPLC purity: 99.78%.

#### 4.4.9. 3-Hydroxy-2-methyl-1-(2-(prop-2-yn-1-yl(3-(trifluoromethyl)benzyl)amino)ethyl)pyridin-4(1H)-one (6i)

Yield: 84%, white solid, m.p. 133.8–135.7 °C,  $^1\text{H}$  NMR (400 MHz,  $\text{DMSO}-d_6$ )  $\delta$  10.45 (br, 1H), 8.15 (d,  $J = 7.0$  Hz, 1H), 7.61 (d,  $J = 7.4$  Hz, 1H), 7.54 (s, 1H), 7.46–7.40 (m, 2H), 7.31 (d,  $J = 6.9$  Hz, 1H), 4.54 (d,  $J = 6.2$  Hz, 2H), 3.87 (s, 2H), 3.62 (s, 2H), 3.41 (s, 1H), 3.00 (br, 2H), 2.39 (s, 3H).  $^{13}\text{C}$  NMR (100 MHz,  $\text{DMSO}-d_6$ )  $\delta$  159.2, 152.2, 143.4, 142.2, 139.2, 134.1, 129.9, 129.6 (q,  $^2J_{\text{C-F}} = 31.4$  Hz), 128.6, 125.9 (d,  $^2J_{\text{C-F}} = 130.2$  Hz), 124.5 (d,  $^1J_{\text{C-F}} = 270.7$  Hz), 110.9, 78.9, 77.0, 56.9, 52.7, 51.3, 42.2, 13.1. HRMS (ESI):  $m/z$  calcd for  $\text{C}_{19}\text{H}_{20}\text{F}_3\text{N}_2\text{O}_2$  [ $\text{M} + \text{H}$ ] $^+$ : 365.1471 found 365.1470. HPLC purity: 99.57%.

#### 4.4.10. 3-Hydroxy-2-methyl-1-(2-(prop-2-yn-1-yl(4-(trifluoromethyl)benzyl)amino)ethyl)pyridin-4(1H)-one (6j)

Yield: 85%, white solid, m.p. 178.6–180.1 °C,  $^1\text{H}$  NMR (400 MHz,  $\text{DMSO}-d_6$ )  $\delta$  10.49 (br, 1H), 8.11 (dd,  $J = 7.0$ , 1.8 Hz, 1H), 7.56 (d,  $J = 8.0$  Hz, 2H), 7.26 (dd,  $J = 8.6$ , 5.0 Hz, 3H), 4.48 (t,  $J = 5.7$  Hz, 2H), 3.75 (s, 2H), 3.55 (s, 2H), 3.33 (s, 1H), 2.87 (br, 2H), 2.36 (s, 3H).  $^{13}\text{C}$  NMR

(100 MHz, DMSO- $d_6$ )  $\delta$  159.3, 143.4, 142.3, 139.2, 130.9, 129.2 (q,  $^2J_{C-F}$  = 31.7 Hz), 125.7 (d,  $^4J_{C-F}$  = 3.6 Hz), 124.6 (d,  $^1J_{C-F}$  = 270.5 Hz), 120.5, 111.0, 79.3, 76.7, 56.8, 52.5, 51.3, 42.2, 13.1. HRMS (ESI):  $m/z$  calcd for  $C_{19}H_{20}F_3N_2O_2$  [M + H] $^+$ : 365.1471 found 365.1473. HPLC purity: 100%.

#### 4.4.11. 1-(2-((2,5-Difluorobenzyl)(prop-2-yn-1-yl)amino)ethyl)-3-hydroxy-2-methylpyridin-4(1H)-one (6k)

Yield: 75%, white solid, m.p. 171.6–173.4 °C,  $^1H$  NMR (400 MHz, DMSO- $d_6$ )  $\delta$  10.41 (br, 1H), 8.05 (d,  $J$  = 7.0 Hz, 1H), 7.24 (d,  $J$  = 7.0 Hz, 1H), 7.14–7.00 (m, 2H), 6.85–6.72 (m, 1H), 4.44 (t,  $J$  = 5.6 Hz, 2H), 3.64 (s, 2H), 3.59 (d,  $J$  = 2.4 Hz, 2H), 3.30 (d,  $J$  = 2.4 Hz, 1H), 2.86 (t,  $J$  = 5.6 Hz, 2H), 2.37 (s, 3H).  $^{13}C$  NMR (100 MHz, DMSO- $d_6$ )  $\delta$  158.9, 158.3 (d,  $^1J_{C-F}$  = 239.2 Hz), 157.2 (d,  $^1J_{C-F}$  = 240.1 Hz), 143.2, 141.8, 139.2, 117.5, 117.3, 117.1 (d,  $^3J_{C-F}$  = 8.8 Hz), 116.3 (dd,  $^2J_{C-F}$  = 32.1 Hz,  $^3J_{C-F}$  = 8.8 Hz), 110.5, 78.7, 77.3, 53.7, 51.2, 50.7, 42.5, 12.9. HRMS (ESI):  $m/z$  calcd for  $C_{18}H_{19}F_2N_2O_2$  [M + H] $^+$ : 333.1409 found 333.1373. HPLC purity: 100%.

#### 4.4.12. 1-(2-((3,5-Difluorobenzyl)(prop-2-yn-1-yl)amino)ethyl)-3-hydroxy-2-methylpyridin-4(1H)-one (6l)

Yield: 70%, white solid, m.p. 164.3–166.1 °C,  $^1H$  NMR (400 MHz, DMSO- $d_6$ )  $\delta$  10.47 (br, 1H), 8.13 (d,  $J$  = 7.0 Hz, 1H), 7.32 (d,  $J$  = 6.9 Hz, 1H), 7.06 (tt,  $J$  = 9.2, 2.3 Hz, 1H), 6.78 (d,  $J$  = 7.3 Hz, 2H), 4.51 (t,  $J$  = 5.6 Hz, 2H), 3.73 (s, 2H), 3.69–3.61 (m, 2H), 3.37 (d,  $J$  = 3.0 Hz, 1H), 2.92 (br, 2H), 2.39 (s, 3H).  $^{13}C$  NMR (100 MHz, DMSO- $d_6$ )  $\delta$  162.6 (dd,  $^1J_{C-F}$  = 244.7 Hz,  $^3J_{C-F}$  = 13.1 Hz), 163.8, 161.5, 161.3, 159.1, 143.3, 142.0, 139.2, 137.7, 112.6 (d,  $^2J_{C-F}$  = 24.0 Hz), 112.5, 110.7, 103.8 (t,  $^2J_{C-F}$  = 26.1 Hz), 78.6, 77.4, 56.8, 52.9, 51.0, 42.3, 13.0. HRMS (ESI):  $m/z$  calcd for  $C_{18}H_{19}F_2N_2O_2$  [M + H] $^+$ : 333.1409 found 333.1408. HPLC purity: 99.34%.

#### 4.4.13. 3-Hydroxy-2-methyl-1-(2-((3-methylbenzyl)(prop-2-yn-1-yl)amino)ethyl)pyridin-4(1H)-one (6m)

Yield: 66%, white solid, m.p. 185.5–187.2 °C,  $^1H$  NMR (400 MHz, DMSO- $d_6$ )  $\delta$  10.51 (br, 1H), 8.24 (d,  $J$  = 6.9 Hz, 1H), 7.40 (d,  $J$  = 6.8 Hz, 1H), 7.18 (dd,  $J$  = 23.0, 6.6 Hz, 4H), 4.73 (t,  $J$  = 5.6 Hz, 2H), 4.03 (s, 2H), 3.81 (s, 2H), 3.67 (s, 1H), 3.25 (br, 2H), 2.43 (s, 3H), 2.25 (s, 3H).  $^{13}C$  NMR (100 MHz, DMSO- $d_6$ )  $\delta$  159.3, 143.4, 142.4, 139.2, 138.3, 133.1, 131.2, 129.8, 128.9, 127.8, 111.1, 80.4, 75.5, 57.3, 51.8, 50.7, 42.1, 21.4, 13.2. HRMS (ESI):  $m/z$  calcd for  $C_{19}H_{23}N_2O_2$  [M + H] $^+$ : 311.1754 found 311.1747. HPLC purity: 98.55%.

#### 4.4.14. 3-Hydroxy-2-methyl-1-(2-((4-methylbenzyl)(prop-2-yn-1-yl)amino)ethyl)pyridin-4(1H)-one (6n)

Yield: 65%, white solid, m.p. 155.6–157.4 °C,  $^1H$  NMR (400 MHz, DMSO- $d_6$ )  $\delta$  10.48 (br, 1H), 8.11 (d,  $J$  = 4.8 Hz, 1H), 7.30 (d,  $J$  = 6.4 Hz, 1H), 7.05 (s, 4H), 4.56 (br, 2H), 3.78 (s, 2H), 3.65 (s, 2H), 3.43 (s, 2H), 3.02 (br, 2H), 2.37 (s, 3H), 2.28 (s, 3H).  $^{13}C$  NMR (100 MHz, DMSO- $d_6$ )  $\delta$  159.4, 143.5, 142.4, 139.1, 138.9, 138.8, 130.8, 129.6, 111.2, 80.8, 75.1, 51.7, 50.8, 42.0, 21.3, 13.3. HRMS (ESI):  $m/z$  calcd for  $C_{19}H_{23}N_2O_2$  [M + H] $^+$ : 311.1754 found 311.1744. HPLC purity: 98.63%.

#### 4.4.15. 3-Hydroxy-2-methyl-1-(2-(methyl(prop-2-yn-1-yl)amino)ethyl)pyridin-4(1H)-one (6o)

Yield: 60%, white solid, m.p. 201.3–202.7 °C,  $^1H$  NMR (400 MHz, DMSO- $d_6$ )  $\delta$  10.57 (br, 1H), 8.32 (d,  $J$  = 7.1 Hz, 1H), 7.36 (d,  $J$  = 7.0 Hz, 1H), 4.81 (t,  $J$  = 7.6 Hz, 2H), 4.12 (s, 2H), 3.83 (s, 1H), 3.48 (t,  $J$  = 7.6 Hz, 2H), 2.81 (s, 3H), 2.58 (s, 3H).  $^{13}C$  NMR (100 MHz, DMSO- $d_6$ )  $\delta$  159.8, 143.6, 142.4, 139.1, 111.4, 82.0, 73.6, 52.4, 50.3, 45.2, 39.8, 13.5. HRMS (ESI):  $m/z$  calcd for  $C_{12}H_{17}N_2O_2$  [M + H] $^+$ : 221.1285 found 221.1278. HPLC purity: 98.82%.

### 4.5. Preparation method of intermediate 9

A mixture of kojic acid **7** (5 mmol), benzyl bromide (7.5 mmol), and anhydrous  $K_2CO_3$  (7.5 mmol) in  $H_2O$ /ethanol (20 mL) reacted for 2 h. The solvent was removed, and then the crude material was washed with water and petroleum ether to afford white solid **8**. Then, intermediate **8** (5 mmol), methylamine (40% in water, 6 mmol) and NaOH (10 mmol) were dissolved in ethyl alcohol/ $H_2O$  (1:1), and the reaction was heated at reflux for 1 h. The solvent was removed and the residue was purified by column chromatography with DCM/MeOH (25:1) to afford intermediate **9** as a reddish-brown solid.

#### 4.5.1. 5-(Benzyloxy)-2-(hydroxymethyl)-1-methylpyridin-4(1H)-one (9)

Yield: 95%, white solid, m.p. 215.2–216.9 °C,  $^1H$  NMR (400 MHz, DMSO- $d_6$ )  $\delta$  8.72 (s, 1H), 7.50 (d,  $J$  = 2.1 Hz, 2H), 7.48 (d,  $J$  = 1.5 Hz, 1H), 7.48–7.36 (m, 3H), 5.22 (s, 2H), 5.09 (s, 2H), 4.12 (s, 3H).

### 4.6. Preparation method of intermediate 10

A solution of intermediate **9** (2 mmol) in  $SOCl_2$  (5 mL) was allowed to stir at room temperature for 1 h. The solvent was removed in vacuo. The crude material was recrystallized with methanol/ether to give intermediate **10** as a gray solid.

#### 4.6.1. 5-(Benzyloxy)-2-(chloromethyl)-1-methylpyridin-4(1H)-one (10)

Yield: 95%, yellow solid, m.p. 165.1–167.0 °C,  $^1H$  NMR (400 MHz,  $CDCl_3$ )  $\delta$  7.40–7.36 (m, 2H), 7.35–7.27 (m, 3H), 7.05 (s, 1H), 6.47 (s, 1H), 5.12 (s, 2H), 4.35 (s, 2H), 3.65 (s, 3H).

### 4.7. Preparation method of intermediates 12a-n

Solution of compounds **11a-n** (4 mmol) and  $K_2CO_3$  (3 mmol) in DMF (15 mL) stirred at room temperature for fifteen minutes, and 3-bromopropyne (2 mmol) in DMF (10 mL) was added and followed by stirring for another 12 h. Upon completion of the reaction, the solvents were removed, then the crude products were purified by column chromatography (*n*-hexane:ethyl acetate = 7:1) to afford intermediate **12a-n** as yellow oils.

#### 4.7.1. N-benzylprop-2-yn-1-amine (12a)

Yield: 70%, yellow oil.  $^1H$  NMR (400 MHz,  $CDCl_3$ )  $\delta$  7.36 (td,  $J$  = 7.6, 1.8 Hz, 1H), 7.30–7.20 (m, 1H), 7.13–7.01 (m, 2H), 3.93 (s, 2H), 3.44 (d,  $J$  = 2.5 Hz, 2H), 2.26 (t,  $J$  = 2.5 Hz, 1H).

#### 4.7.2. N-(2-chlorobenzyl)prop-2-yn-1-amine (12b)

Yield: 65%, yellow oil.  $^1H$  NMR (400 MHz,  $CDCl_3$ )  $\delta$  7.46–7.42 (m, 1H), 7.41–7.37 (m, 1H), 7.25 (m, 2H), 4.01 (s, 2H), 3.48 (d,  $J$  = 2.5 Hz, 2H), 2.30 (t,  $J$  = 2.5 Hz, 1H).

#### 4.7.3. N-(3-chlorobenzyl)prop-2-yn-1-amine (12c)

Yield: 66%, yellow oil.  $^1H$  NMR (400 MHz,  $CDCl_3$ )  $\delta$  7.39 (d,  $J$  = 2.0 Hz, 1H), 7.33–7.21 (m, 3H), 3.89 (s, 2H), 3.45 (d,  $J$  = 2.4 Hz, 2H), 2.29 (t,  $J$  = 2.4 Hz, 1H).

#### 4.7.4. N-(4-chlorobenzyl)prop-2-yn-1-amine (12d)

Yield: 71%, yellow oil.  $^1H$  NMR (400 MHz,  $CDCl_3$ )  $\delta$  7.29 (s, 4H), 3.85 (s, 2H), 3.41 (d,  $J$  = 2.4 Hz, 2H), 2.26 (t,  $J$  = 2.4 Hz, 1H).

#### 4.7.5. N-(2-fluorobenzyl)prop-2-yn-1-amine (12e)

Yield: 70%, yellow oil.  $^1H$  NMR (400 MHz,  $CDCl_3$ )  $\delta$  7.39 (td,  $J$  = 7.6, 1.8 Hz, 1H), 7.32–7.23 (m, 1H), 7.16–7.03 (m, 2H), 3.96 (d,  $J$  = 1.0 Hz, 2H), 3.47 (d,  $J$  = 2.4 Hz, 2H), 2.28 (t,  $J$  = 2.4 Hz, 1H).

#### 4.7.6. N-(3-fluorobenzyl)prop-2-yn-1-amine (12f)

Yield: 75%, yellow oil.  $^1H$  NMR (400 MHz,  $CDCl_3$ )  $\delta$  7.33–7.25 (m, 1H), 7.15–7.04 (m, 2H), 7.00–6.91 (m, 1H), 3.89 (s, 2H), 3.43 (d,  $J$  =

2.4 Hz, 2H), 2.27 (t,  $J = 2.4$  Hz, 1H).

#### 4.7.7. *N*-(4-fluorobenzyl)prop-2-yn-1-amine (**12g**)

Yield: 60%, yellow oil.  $^1\text{H NMR}$  (400 MHz,  $\text{CDCl}_3$ )  $\delta$  7.38–7.31 (m, 2H), 7.07–7.00 (m, 2H), 3.88 (s, 2H), 3.44 (d,  $J = 2.4$  Hz, 2H), 2.29 (t,  $J = 2.4$  Hz, 1H).

#### 4.7.8. *N*-(2-methoxybenzyl)prop-2-yn-1-amine (**12h**)

Yield: 65%, yellow oil.  $^1\text{H NMR}$  (600 MHz,  $\text{CDCl}_3$ )  $\delta$  7.27 (t,  $J = 1.5$  Hz, 1H), 7.27–7.22 (m, 1H), 6.92 (td,  $J = 7.4, 1.1$  Hz, 1H), 6.87 (d,  $J = 8.1$  Hz, 1H), 3.89 (s, 2H), 3.85 (s, 3H), 3.42 (d,  $J = 2.5$  Hz, 2H), 2.24 (t,  $J = 2.5$  Hz, 1H).

#### 4.7.9. *N*-(3-methoxybenzyl)prop-2-yn-1-amine (**12i**)

Yield: 71%, yellow oil.  $^1\text{H NMR}$  (400 MHz,  $\text{CDCl}_3$ )  $\delta$  7.47–7.40 (m, 2H), 7.39–7.35 (m, 1H), 7.25 (td,  $J = 7.6, 0.9$  Hz, 1H), 3.81 (s, 3H), 3.66 (s, 2H), 3.28 (d,  $J = 2.4$  Hz, 2H), 2.34 (t,  $J = 2.4$  Hz, 1H).

#### 4.7.10. *N*-(4-methoxybenzyl)prop-2-yn-1-amine (**12j**)

Yield: 72%, yellow oil.  $^1\text{H NMR}$  (400 MHz,  $\text{CDCl}_3$ )  $\delta$  7.27 (d,  $J = 8.4$  Hz, 2H), 6.89–6.84 (m, 2H), 3.82 (s, 2H), 3.80 (s, 3H), 3.41 (d,  $J = 2.4$  Hz, 2H), 2.26 (t,  $J = 2.4$  Hz, 1H).

#### 4.7.11. *N*-(2-methylbenzyl)prop-2-yn-1-amine (**12k**)

Yield: 73%, yellow oil.  $^1\text{H NMR}$  (400 MHz,  $\text{CDCl}_3$ )  $\delta$  7.29–7.32 (m, 1H), 7.17 (d,  $J = 3.3$  Hz, 3H), 3.88 (s, 2H), 3.47 (d,  $J = 2.4$  Hz, 2H), 2.38 (s, 3H), 2.28 (t,  $J = 2.4$  Hz, 1H).

#### 4.7.12. *N*-(4-methylbenzyl)prop-2-yn-1-amine (**12l**)

Yield: 61%, yellow oil.  $^1\text{H NMR}$  (400 MHz,  $\text{CDCl}_3$ )  $\delta$  7.25–7.22 (m, 2H), 7.14 (d,  $J = 7.8$  Hz, 2H), 3.85 (s, 2H), 3.42 (d,  $J = 2.4$  Hz, 2H), 2.34 (s, 3H), 2.26 (t,  $J = 2.4$  Hz, 1H).

#### 4.7.13. *N*-(4-(trifluoromethyl)benzyl)prop-2-yn-1-amine (**12m**)

Yield: 65%, yellow oil.  $^1\text{H NMR}$  (400 MHz,  $\text{CDCl}_3$ )  $\delta$  7.61 (d,  $J = 8.1$  Hz, 2H), 7.50 (d,  $J = 7.4$  Hz, 2H), 3.98 (s, 2H), 3.46 (d,  $J = 2.4$  Hz, 2H), 2.30 (t,  $J = 2.4$  Hz, 1H).

#### 4.7.14. *N*-(3,5-difluorobenzyl)prop-2-yn-1-amine (**12n**)

Yield: 66%, yellow oil.  $^1\text{H NMR}$  (400 MHz,  $\text{CDCl}_3$ )  $\delta$  6.95–6.85 (m, 2H), 6.68 (tt,  $J = 9.0, 2.4$  Hz, 1H), 3.86 (s, 2H), 3.41 (d,  $J = 2.4$  Hz, 2H), 2.26 (t,  $J = 2.4$  Hz, 1H).

### 4.8. Preparation method of intermediates **13a-n**

A mixture of intermediates **10** (1.3 mmol), compounds **12a-n** (1.1 mmol) and triethylamine (2 mmol) in acetonitrile (25 mL) reacted for 20 h. The solvents were concentrated and then the crude material was purified by column chromatography (DCM: MeOH = 30:1–15:1, gradient elution) to afford intermediate **13a-n** as yellow oils.

#### 4.8.1. 2-((Benzyl(prop-2-yn-1-yl)amino)methyl)-5-(benzyloxy)-1-methylpyridin-4(1H)-one (**13a**)

Yield: 75%, yellow oil.  $^1\text{H NMR}$  (400 MHz,  $\text{CDCl}_3$ )  $\delta$  7.43–7.38 (m, 2H), 7.39–7.27 (m, 4H), 7.28 (d,  $J = 4.1$  Hz, 4H), 6.90 (s, 1H), 6.55 (s, 1H), 5.17 (s, 2H), 3.66 (s, 2H), 3.53 (s, 3H), 3.51 (s, 2H), 3.25 (d,  $J = 2.4$  Hz, 2H), 2.32 (t,  $J = 2.4$  Hz, 1H).

#### 4.8.2. 5-(Benzyloxy)-2-(((2-chlorobenzyl)(prop-2-yn-1-yl)amino)methyl)-1-methyl pyridin-4(1H)-one (**13b**)

Yield: 80%, yellow oil.  $^1\text{H NMR}$  (400 MHz,  $\text{CDCl}_3$ )  $\delta$  7.40 (d,  $J = 1.8$  Hz, 1H), 7.40–7.37 (m, 2H), 7.34 (td,  $J = 4.2, 3.4, 1.5$  Hz, 3H), 7.32–7.27 (m, 1H), 7.25–7.18 (m, 2H), 6.89 (s, 1H), 6.54 (s, 1H), 5.16 (s, 2H), 3.74 (s, 2H), 3.54 (s, 2H), 3.51 (s, 3H), 3.25 (t,  $J = 2.4$  Hz, 2H), 2.36 (t,  $J = 2.4$  Hz, 1H).

#### 4.8.3. 5-(Benzyloxy)-2-(((3-chlorobenzyl)(prop-2-yn-1-yl)amino)methyl)-1-methyl pyridin-4(1H)-one (**13c**)

Yield: 82%, yellow oil.  $^1\text{H NMR}$  (400 MHz,  $\text{CDCl}_3$ )  $\delta$  7.47–7.29 (m, 5H), 7.30–7.22 (m, 3H), 7.18 (ddd,  $J = 4.9, 3.5, 1.8$  Hz, 1H), 6.94 (s, 1H), 6.56 (s, 1H), 5.19 (s, 2H), 3.66 (s, 2H), 3.60 (s, 3H), 3.54 (s, 2H), 3.27 (d,  $J = 2.4$  Hz, 2H), 2.36 (t,  $J = 2.4$  Hz, 1H).

#### 4.8.4. 5-(Benzyloxy)-2-(((4-chlorobenzyl)(prop-2-yn-1-yl)amino)methyl)-1-methyl pyridin-4(1H)-one (**13d**)

Yield: 86%, yellow oil.  $^1\text{H NMR}$  (400 MHz,  $\text{CDCl}_3$ )  $\delta$  7.42–7.37 (m, 2H), 7.35–7.31 (m, 2H), 7.31–7.27 (m, 2H), 7.25 (d,  $J = 2.4$  Hz, 1H), 7.20 (d,  $J = 2.2$  Hz, 1H), 7.19 (d,  $J = 1.9$  Hz, 1H), 7.11 (s, 1H), 6.54 (s, 1H), 5.14 (s, 2H), 3.62 (s, 2H), 3.61 (s, 3H), 3.51 (s, 2H), 3.20 (d,  $J = 2.4$  Hz, 2H), 2.32 (t,  $J = 2.4$  Hz, 1H).

#### 4.8.5. 5-(Benzyloxy)-2-(((2-fluorobenzyl)(prop-2-yn-1-yl)amino)methyl)-1-methyl pyridin-4(1H)-one (**13e**)

Yield: 85%, yellow oil.  $^1\text{H NMR}$  (400 MHz,  $\text{CDCl}_3$ )  $\delta$  7.45–7.40 (m, 2H), 7.40–7.33 (m, 2H), 7.33–7.30 (m, 3H), 7.11 (td,  $J = 7.5, 1.1$  Hz, 1H), 7.04 (ddd,  $J = 9.4, 8.0, 1.1$  Hz, 1H), 6.93 (s, 1H), 6.55 (s, 1H), 5.18 (s, 2H), 3.73 (s, 2H), 3.57 (s, 2H), 3.56 (s, 3H), 3.26 (d,  $J = 2.4$  Hz, 2H), 2.37 (t,  $J = 2.4$  Hz, 1H).

#### 4.8.6. 5-(Benzyloxy)-2-(((3-fluorobenzyl)(prop-2-yn-1-yl)amino)methyl)-1-methyl pyridin-4(1H)-one (**13f**)

Yield: 78%, yellow oil.  $^1\text{H NMR}$  (400 MHz,  $\text{CDCl}_3$ )  $\delta$  7.42–7.38 (m, 2H), 7.37–7.31 (m, 2H), 7.29 (dd,  $J = 7.4, 1.9$  Hz, 1H), 7.25 (s, 1H), 7.05 (dt,  $J = 7.6, 1.2$  Hz, 1H), 7.01–6.93 (m, 2H), 6.92 (s, 1H), 6.53 (s, 1H), 5.17 (s, 2H), 3.65 (s, 2H), 3.58 (s, 3H), 3.52 (s, 2H), 3.24 (d,  $J = 2.4$  Hz, 2H), 2.33 (t,  $J = 2.4$  Hz, 1H).

#### 4.8.7. 5-(Benzyloxy)-2-(((4-fluorobenzyl)(prop-2-yn-1-yl)amino)methyl)-1-methyl pyridin-4(1H)-one (**13g**)

Yield: 80%, yellow oil.  $^1\text{H NMR}$  (400 MHz,  $\text{CDCl}_3$ )  $\delta$  7.44–7.38 (m, 2H), 7.34 (t,  $J = 7.1$  Hz, 2H), 7.25–7.21 (m, 2H), 7.00 (td,  $J = 8.6, 3.7$  Hz, 3H), 6.91 (s, 1H), 6.54 (s, 1H), 5.17 (s, 2H), 3.63 (s, 2H), 3.55 (s, 3H), 3.51 (s, 2H), 3.23 (d,  $J = 2.4$  Hz, 2H), 2.33 (t,  $J = 2.4$  Hz, 1H).

#### 4.8.8. 5-(Benzyloxy)-2-(((2-methoxybenzyl)(prop-2-yn-1-yl)amino)methyl)-1-methyl pyridin-4(1H)-one (**13h**)

Yield: 75%, yellow oil.  $^1\text{H NMR}$  (400 MHz,  $\text{CDCl}_3$ )  $\delta$  7.45–7.40 (m, 2H), 7.36–7.31 (m, 3H), 7.28 (m, 2H), 7.21 (t,  $J = 7.0$  Hz, 1H), 7.14 (d,  $J = 1.1$  Hz, 1H), 6.96 (s, 1H), 6.60 (s, 1H), 5.20 (s, 2H), 3.80 (s, 3H), 3.69 (s, 2H), 3.60 (s, 3H), 3.50 (s, 2H), 3.30 (d,  $J = 2.4$  Hz, 2H), 2.35 (t,  $J = 2.4$  Hz, 1H).

#### 4.8.9. 5-(Benzyloxy)-2-(((3-methoxybenzyl)(prop-2-yn-1-yl)amino)methyl)-1-methyl pyridin-4(1H)-one (**13i**)

Yield: 70%, yellow oil.  $^1\text{H NMR}$  (400 MHz,  $\text{CDCl}_3$ )  $\delta$  7.35–7.40 (m, 2H), 7.34 (s, 2H), 7.30–7.28 (m, 1H), 7.23 (m, 1H), 7.15 (ddd,  $J = 7.5, 1.8, 0.9$  Hz, 1H), 6.86 (s, 1H), 6.82 (m, 1H), 6.80 (s, 1H), 6.50 (s, 1H), 5.12 (s, 2H), 3.79 (s, 3H), 3.77 (s, 2H), 3.69 (s, 2H), 3.64 (d,  $J = 2.4$  Hz, 2H), 3.25 (s, 3H), 2.37 (t,  $J = 2.4$  Hz, 1H).

#### 4.8.10. 5-(Benzyloxy)-2-(((4-methoxybenzyl)(prop-2-yn-1-yl)amino)methyl)-1-methyl pyridin-4(1H)-one (**13j**)

Yield: 66%, yellow oil.  $^1\text{H NMR}$  (400 MHz,  $\text{CDCl}_3$ )  $\delta$  7.46–7.42 (m, 2H), 7.38–7.32 (m, 3H), 7.25 (dd,  $J = 7.1, 1.7$  Hz, 2H), 7.00 (s, 1H), 6.95–6.84 (m, 2H), 6.56 (s, 1H), 5.19 (s, 2H), 3.75 (s, 3H), 3.69 (s, 2H), 3.58 (s, 3H), 3.56 (s, 2H), 3.27 (d,  $J = 2.4$  Hz, 2H), 2.34 (t,  $J = 2.4$  Hz, 1H).

#### 4.8.11. 5-(Benzyloxy)-1-methyl-2-(((2-methylbenzyl)(prop-2-yn-1-yl)amino)methyl) pyridin-4(1H)-one (**13k**)

Yield: 80%, yellow oil.  $^1\text{H NMR}$  (400 MHz,  $\text{CDCl}_3$ )  $\delta$  7.44–7.40 (m, 2H), 7.35 (d,  $J = 6.5$  Hz, 1H), 7.34–7.29 (m, 2H), 7.28 (s, 1H), 7.23 (d,  $J = 2.4$  Hz, 1H).

= 2.2 Hz, 1H), 7.21 (d,  $J = 2.0$  Hz, 1H), 7.13 (s, 1H), 6.56 (s, 1H), 5.18 (s, 2H), 3.65 (s, 2H), 3.54 (s, 3H), 3.49 (s, 2H), 3.23 (d,  $J = 2.4$  Hz, 2H), 2.33 (s, 3H), 2.33 (t,  $J = 2.4$  Hz, 2H).

#### 4.8.12. 5-(Benzyloxy)-1-methyl-2-((4-methylbenzyl)(prop-2-yn-1-yl)amino)methylpyridin-4(1H)-one (13l)

Yield: 75%, yellow oil.  $^1\text{H NMR}$  (400 MHz,  $\text{CDCl}_3$ )  $\delta$  7.43–7.38 (m, 2H), 7.36–7.32 (m, 2H), 7.32–7.27 (m, 1H), 7.19–7.08 (m, 5H), 6.93 (s, 1H), 6.55 (s, 1H), 5.17 (s, 2H), 3.61 (s, 2H), 3.54 (s, 3H), 3.49 (s, 2H), 3.23 (d,  $J = 2.5$  Hz, 2H), 2.33 (s, 3H), 2.31 (t,  $J = 2.5$  Hz, 2H).

#### 4.8.13. 5-(Benzyloxy)-1-methyl-2-((prop-2-yn-1-yl(4-(trifluoromethyl)benzyl)amino)methyl)pyridin-4(1H)-one (13m)

Yield: 76%, yellow oil.  $^1\text{H NMR}$  (400 MHz,  $\text{CDCl}_3$ )  $\delta$  7.60 (d,  $J = 8.0$  Hz, 2H), 7.45–7.39 (m, 4H), 7.39–7.30 (m, 3H), 6.99 (s, 1H), 6.60 (s, 1H), 5.19 (s, 2H), 3.74 (s, 2H), 3.63 (s, 3H), 3.57 (s, 2H), 3.26 (d,  $J = 2.4$  Hz, 2H), 2.37 (t,  $J = 2.4$  Hz, 1H).

#### 4.8.14. 5-(Benzyloxy)-2-((3,5-difluorobenzyl)(prop-2-yn-1-yl)amino)methyl-1-methylpyridin-4(1H)-one (13n)

Yield: 77%, yellow oil.  $^1\text{H NMR}$  (400 MHz,  $\text{CDCl}_3$ )  $\delta$  7.44–7.39 (m, 2H), 7.33 (dt,  $J = 13.4, 6.8$  Hz, 3H), 6.93 (s, 1H), 6.83–6.78 (m, 2H), 6.76–6.66 (m, 1H), 6.53 (s, 1H), 5.17 (s, 2H), 3.64 (s, 2H), 3.62 (s, 3H), 3.54 (s, 2H), 3.24 (d,  $J = 2.4$  Hz, 2H), 2.34 (t,  $J = 2.4$  Hz, 1H).

### 4.9. Preparation method of compounds 14a-n

Intermediate **13a-o** (1 mmol) were completely dissolved in anhydrous DCM (10 mL), then 3 mL of  $\text{BCl}_3$  solution (1 mmol/L DCM) was added to the solution at  $-20$  °C, and the reaction was carried out under nitrogen protection. After the addition, the reaction system was continuously stirred for 2 h, quenched with methanol (15 mL), warmed to room temperature and stirred for 12 h. The solvent was concentrated and the obtained crude material was purified by recrystallization (methanol/ether) to obtain **14a-n** as white solids.

#### 4.9.1. 2-((Benzyl(prop-2-yn-1-yl)amino)methyl)-5-hydroxy-1-methylpyridin-4(1H)-one (14a)

Yield: 80%, white solid, m.p. 173.6–175.2 °C,  $^1\text{H NMR}$  (400 MHz,  $\text{DMSO}-d_6$ )  $\delta$  11.12 (br, 1H), 8.28 (s, 1H), 7.42 (s, 1H), 7.33 (d,  $J = 4.4$  Hz, 3H), 7.31–7.24 (m, 1H), 4.04 (s, 3H), 3.86 (s, 2H), 3.70 (s, 2H), 3.38 (t,  $J = 2.4$  Hz, 1H), 3.27 (d,  $J = 2.4$  Hz, 2H).  $^{13}\text{C NMR}$  (100 MHz,  $\text{DMSO}-d_6$ )  $\delta$  160.3, 146.3, 144.7, 137.5, 134.0, 129.5, 128.9, 128.0, 114.7, 77.9, 65.4, 57.5, 53.9, 43.5, 41.8. HRMS (ESI):  $m/z$  calcd for  $\text{C}_{17}\text{H}_{19}\text{N}_2\text{O}_2$  [ $\text{M} + \text{H}$ ] $^+$ : 283.1441 found 283.1438. HPLC purity: 99.60%.

#### 4.9.2. 2-(((2-Chlorobenzyl)(prop-2-yn-1-yl)amino)methyl)-5-hydroxy-1-methylpyridin-4(1H)-one (14b)

Yield: 81%, white solid, m.p. 190.1–191.6 °C,  $^1\text{H NMR}$  (400 MHz,  $\text{DMSO}-d_6$ )  $\delta$  11.17 (br, 1H), 8.29 (s, 1H), 7.49–7.40 (m, 2H), 7.36–7.28 (m, 2H), 4.02 (s, 3H), 3.89 (s, 2H), 3.77 (s, 2H), 3.42 (t,  $J = 2.4$  Hz, 1H), 3.31 (d,  $J = 2.4$  Hz, 2H).  $^{13}\text{C NMR}$  (100 MHz,  $\text{DMSO}-d_6$ )  $\delta$  160.2, 146.2, 144.7, 135.1, 134.1, 134.0, 131.9, 130.0, 129.9, 127.7, 115.0, 78.0, 78.0, 54.3, 54.1, 43.4, 42.0. HRMS (ESI):  $m/z$  calcd for  $\text{C}_{17}\text{H}_{18}\text{ClN}_2\text{O}_2$  [ $\text{M} + \text{H}$ ] $^+$ : 317.1051 found 317.1056. HPLC purity: 99.50%.

#### 4.9.3. 2-(((3-Chlorobenzyl)(prop-2-yn-1-yl)amino)methyl)-5-hydroxy-1-methylpyridin-4(1H)-one (14c)

Yield: 85%, white solid, m.p. 177.5–179.2 °C,  $^1\text{H NMR}$  (400 MHz,  $\text{DMSO}-d_6$ )  $\delta$  11.16 (br, 1H), 8.29 (s, 1H), 7.40 (s, 1H), 7.38–7.28 (m, 3H), 4.05 (s, 3H), 3.86 (s, 2H), 3.71 (s, 2H), 3.41 (t,  $J = 2.4$  Hz, 1H), 3.29 (d,  $J = 2.4$  Hz, 2H).  $^{13}\text{C NMR}$  (100 MHz,  $\text{DMSO}-d_6$ )  $\delta$  160.2, 146.2, 144.7, 140.4, 134.0, 133.5, 130.8, 129.1, 128.1, 128.0, 114.7, 80.2, 78.0, 56.9, 54.0, 43.5, 41.9. HRMS (ESI):  $m/z$  calcd for  $\text{C}_{17}\text{H}_{18}\text{ClN}_2\text{O}_2$  [ $\text{M} + \text{H}$ ] $^+$ : 317.1051 found 317.1050. HPLC purity: 99.78%.

#### 4.9.4. 2-(((4-Chlorobenzyl)(prop-2-yn-1-yl)amino)methyl)-5-hydroxy-1-methylpyridin-4(1H)-one (14d)

Yield: 86%, white solid, m.p. 188.1–189.8 °C,  $^1\text{H NMR}$  (400 MHz,  $\text{DMSO}-d_6$ )  $\delta$  11.10 (br, 1H), 8.30–8.23 (m, 1H), 7.45–7.33 (m, 6H), 4.03 (s, 3H), 3.84 (s, 2H), 3.68 (s, 2H), 3.38 (t,  $J = 2.4$  Hz, 1H), 3.26 (d,  $J = 2.4$  Hz, 2H).  $^{13}\text{C NMR}$  (100 MHz,  $\text{DMSO}-d_6$ )  $\delta$  160.3, 146.2, 144.7, 136.6, 133.9, 132.6, 131.4, 128.8, 114.7, 78.0, 77.9, 56.6, 53.9, 43.6, 41.8. HRMS (ESI):  $m/z$  calcd for  $\text{C}_{17}\text{H}_{18}\text{ClN}_2\text{O}_2$  [ $\text{M} + \text{H}$ ] $^+$ : 317.1051 found 317.1054. HPLC purity: 100%.

#### 4.9.5. 2-(((2-Fluorobenzyl)(prop-2-yn-1-yl)amino)methyl)-5-hydroxy-1-methylpyridin-4(1H)-one (14e)

Yield: 80%, white solid, m.p. 176.5–178.2 °C,  $^1\text{H NMR}$  (400 MHz,  $\text{DMSO}-d_6$ )  $\delta$  11.17 (br, 1H), 8.29 (s, 1H), 7.45–7.30 (m, 3H), 7.21–7.12 (m, 2H), 4.02 (s, 3H), 3.88 (s, 2H), 3.73 (s, 2H), 3.40 (t,  $J = 2.4$  Hz, 1H), 3.29 (d,  $J = 2.4$  Hz, 2H).  $^{13}\text{C NMR}$  (100 MHz,  $\text{DMSO}$ )  $\delta$  161.3 (d,  $^1J_{\text{C-F}} = 244.1$  Hz), 160.2, 146.2, 144.7, 134.0, 132.0 (d,  $^3J_{\text{C-F}} = 4.1$  Hz), 130.2 (d,  $^3J_{\text{C-F}} = 8.2$  Hz), 124.9 (d,  $^4J_{\text{C-F}} = 3.2$  Hz), 124.5 (d,  $^2J_{\text{C-F}} = 14.0$  Hz), 115.9 (d,  $^2J_{\text{C-F}} = 21.4$  Hz), 114.8, 78.0, 77.9, 54.0, 50.4, 43.3, 41.8. HRMS (ESI):  $m/z$  calcd for  $\text{C}_{17}\text{H}_{18}\text{FN}_2\text{O}_2$  [ $\text{M} + \text{H}$ ] $^+$ : 301.1347 found 301.1346. HPLC purity: 99.38%.

#### 4.9.6. 2-(((3-Fluorobenzyl)(prop-2-yn-1-yl)amino)methyl)-5-hydroxy-1-methylpyridin-4(1H)-one (14f)

Yield: 82%, white solid, m.p. 185.3–187.2 °C,  $^1\text{H NMR}$  (400 MHz,  $\text{DMSO}-d_6$ )  $\delta$  11.15 (br, 1H), 8.28 (s, 1H), 7.43–7.34 (m, 2H), 7.21–7.06 (m, 3H), 4.04 (s, 3H), 3.86 (s, 2H), 3.71 (s, 2H), 3.40 (t,  $J = 2.4$  Hz, 1H), 3.28 (d,  $J = 2.4$  Hz, 2H).  $^{13}\text{C NMR}$  (100 MHz,  $\text{DMSO}-d_6$ )  $\delta$  162.7 (d,  $^1J_{\text{C-F}} = 263.4$  Hz), 160.3, 146.4, 144.6, 140.8 (d,  $^3J_{\text{C-F}} = 7.3$  Hz), 134.0, 130.8 (d,  $^3J_{\text{C-F}} = 8.3$  Hz), 125.4 (d,  $^4J_{\text{C-H}} = 2.4$  Hz), 115.9 (d,  $^2J_{\text{C-F}} = 21.1$ ), 114.8 (d,  $^2J_{\text{C-F}} = 20.9$ ), 114.6, 80.2, 77.9, 56.9, 54.0, 43.5, 41.9. HRMS (ESI):  $m/z$  calcd for  $\text{C}_{17}\text{H}_{18}\text{FN}_2\text{O}_2$  [ $\text{M} + \text{H}$ ] $^+$ : 301.1347 found 301.1349. HPLC purity: 99.94%.

#### 4.9.7. 2-(((4-Fluorobenzyl)(prop-2-yn-1-yl)amino)methyl)-5-hydroxy-1-methylpyridin-4(1H)-one (14g)

Yield: 85%, white solid, m.p. 188.6–190.1 °C,  $^1\text{H NMR}$  (400 MHz,  $\text{DMSO}-d_6$ )  $\delta$  11.16 (br, 1H), 8.29 (s, 1H), 7.42 (s, 1H), 7.41–7.35 (m, 2H), 7.18–7.12 (m, 2H), 4.03 (s, 3H), 3.85 (s, 2H), 3.68 (s, 2H), 3.39 (t,  $J = 2.4$  Hz, 1H), 3.26 (d,  $J = 2.4$  Hz, 2H).  $^{13}\text{C NMR}$  (100 MHz,  $\text{DMSO}-d_6$ )  $\delta$  162.0 (d,  $^1J_{\text{C-F}} = 242$  Hz), 160.3, 146.3, 144.7, 134.0, 133.0, 131.5 (d,  $^3J_{\text{C-F}} = 8.2$  Hz), 115.6 (d,  $^2J_{\text{C-F}} = 21.1$  Hz) 114.7, 80.1, 77.9, 56.6, 53.9, 43.5, 41.8. HRMS (ESI):  $m/z$  calcd for  $\text{C}_{17}\text{H}_{18}\text{FN}_2\text{O}_2$  [ $\text{M} + \text{H}$ ] $^+$ : 301.1347 found 301.1345. HPLC purity: 99.19%.

#### 4.9.8. 5-Hydroxy-2-(((2-methoxybenzyl)(prop-2-yn-1-yl)amino)methyl)-1-methylpyridin-4(1H)-one (14h)

Yield: 86%, white solid, m.p. 136.3–138.2 °C,  $^1\text{H NMR}$  (400 MHz,  $\text{DMSO}-d_6$ )  $\delta$  11.20 (br, 1H), 8.31 (s, 1H), 7.40 (s, 1H), 7.26 (t,  $J = 7.3$  Hz, 2H), 7.02–6.85 (m, 2H), 4.03 (s, 3H), 3.87 (s, 2H), 3.73 (s, 3H), 3.65 (s, 2H), 3.39 (s, 1H), 3.30 (d,  $J = 2.4$  Hz, 2H).  $^{13}\text{C NMR}$  (100 MHz,  $\text{DMSO}-d_6$ )  $\delta$  160.2, 158.0, 146.1, 144.8, 134.0, 131.0, 129.6, 124.9, 120.6, 115.1, 111.4, 78.1, 77.8, 55.8, 54.1, 51.6, 43.4, 42.0. HRMS (ESI):  $m/z$  calcd for  $\text{C}_{18}\text{H}_{21}\text{N}_2\text{O}_3$  [ $\text{M} + \text{H}$ ] $^+$ : 313.1547 found 313.1550. HPLC purity: 100%.

#### 4.9.9. 5-Hydroxy-2-(((3-methoxybenzyl)(prop-2-yn-1-yl)amino)methyl)-1-methylpyridin-4(1H)-one (14i)

Yield: 88%, white solid, m.p. 159.2–161.2 °C,  $^1\text{H NMR}$  (400 MHz,  $\text{DMSO}-d_6$ )  $\delta$  11.13 (br, 1H), 8.27 (s, 1H), 7.39 (s, 1H), 7.24 (t,  $J = 7.8$  Hz, 1H), 6.90 (dt,  $J = 7.5, 1.2$  Hz, 1H), 6.88–6.80 (m, 2H), 4.04 (s, 3H), 3.84 (s, 2H), 3.74 (s, 3H), 3.67 (s, 2H), 3.8 (t,  $J = 2.4$  Hz, 1H), 3.29 (d,  $J = 2.4$  Hz, 2H).  $^{13}\text{C NMR}$  (100 MHz,  $\text{DMSO}-d_6$ )  $\delta$  160.2, 159.8, 146.3, 144.7, 139.2, 133.9, 130.0, 121.6, 114.9, 114.7, 113.4, 78.0, 77.9, 57.6, 55.5, 53.9, 43.5, 42.0. HRMS (ESI):  $m/z$  calcd for  $\text{C}_{18}\text{H}_{21}\text{N}_2\text{O}_3$  [ $\text{M} + \text{H}$ ] $^+$ : 313.1547 found 313.1544. HPLC purity: 99.55%.

#### 4.9.10. 5-Hydroxy-2-(((4-methoxybenzyl)(prop-2-yn-1-yl)amino)methyl)-1-methylpyridin-4(1H)-one (14j)

Yield: 85%, white solid, m.p. 158.6–160.2 °C, <sup>1</sup>H NMR (400 MHz, DMSO-*d*<sub>6</sub>) δ 11.22 (br, 1H), 8.29 (s, 1H), 7.42 (s, 1H), 7.29–7.23 (m, 2H), 6.92–6.85 (m, 2H), 4.03 (s, 3H), 3.85 (s, 2H), 3.73 (s, 3H), 3.65 (s, 2H), 3.39 (t, *J* = 2.4 Hz, 1H), 3.27 (d, *J* = 2.4 Hz, 2H). <sup>13</sup>C NMR (100 MHz, DMSO-*d*<sub>6</sub>) δ 160.2, 159.3, 145.7, 144.7, 134.0, 131.1, 128.6, 115.0, 114.3, 78.3, 77.6, 56.9, 55.6, 53.5, 43.7, 41.6. HRMS (ESI): *m/z* calcd for C<sub>18</sub>H<sub>21</sub>N<sub>2</sub>O<sub>3</sub> [M + H]<sup>+</sup>: 313.1547 found 313.1526 HPLC purity: 96.21%.

#### 4.9.11. 5-Hydroxy-1-methyl-2-(((2-methylbenzyl)(prop-2-yn-1-yl)amino)methyl)pyridine-4(1H)-one (14k)

Yield: 87%, white solid, m.p. 177.4–179.2 °C, <sup>1</sup>H NMR (400 MHz, DMSO-*d*<sub>6</sub>) δ 11.17 (br, 1H), 8.27 (s, 1H), 7.37 (s, 1H), 7.27 (dd, *J* = 7.8, 1.8 Hz, 1H), 7.21–7.11 (m, 3H), 3.97 (s, 3H), 3.84 (s, 2H), 3.68 (s, 2H), 3.41 (t, *J* = 2.4 Hz, 1H), 3.26 (d, *J* = 2.4 Hz, 2H), 2.25 (s, 3H). <sup>13</sup>C NMR (100 MHz, DMSO-*d*<sub>6</sub>) δ 160.2, 146.3, 144.7, 137.7, 135.5, 133.9, 130.8, 130.5, 128.1, 126.2, 114.9, 78.1, 78.0, 55.4, 53.8, 43.3, 41.8, 19.2. HRMS (ESI): *m/z* calcd for C<sub>18</sub>H<sub>21</sub>N<sub>2</sub>O<sub>2</sub> [M + H]<sup>+</sup>: 297.1598 found 297.1599 HPLC purity: 99.85%.

#### 4.9.12. 5-Hydroxy-1-methyl-2-(((4-methylbenzyl)(prop-2-yn-1-yl)amino)methyl)pyridine-4(1H)-one (14l)

Yield: 88%, White solid, m.p. 190.2–192.1 °C, <sup>1</sup>H NMR (400 MHz, DMSO-*d*<sub>6</sub>) δ 11.08 (br, 1H), 8.26 (s, 1H), 7.38 (s, 1H), 7.21 (d, *J* = 8.0 Hz, 2H), 7.13 (d, *J* = 7.8 Hz, 2H), 4.03 (s, 3H), 3.83 (s, 2H), 3.64 (s, 2H), 3.36 (t, *J* = 2.4 Hz, 1H), 3.25 (d, *J* = 2.4 Hz, 2H), 2.28 (s, 3H). <sup>13</sup>C NMR (100 MHz, DMSO-*d*<sub>6</sub>) δ 160.2, 146.4, 144.6, 137.2, 134.5, 134.0, 129.5, 129.5, 114.7, 78.0, 77.9, 57.2, 53.8, 43.5, 41.6, 21.2. HRMS (ESI): *m/z* calcd for C<sub>18</sub>H<sub>21</sub>N<sub>2</sub>O<sub>2</sub> [M + H]<sup>+</sup>: 297.1598 found 297.1581 HPLC purity: 99.68%.

#### 4.9.13. 5-Hydroxy-1-methyl-2-((prop-2-yn-1-yl(4-(trifluoromethyl)benzyl)amino)methyl)pyridin-4(1H)-one (14m)

Yield: 82%, white solid, m.p. 194.6–196.2 °C, <sup>1</sup>H NMR (400 MHz, DMSO-*d*<sub>6</sub>) δ 11.13 (br, 1H), 8.27 (s, 1H), 7.69 (d, *J* = 8.1 Hz, 2H), 7.57 (d, *J* = 8.0 Hz, 2H), 7.41 (s, 1H), 4.05 (s, 3H), 3.89 (s, 2H), 3.80 (s, 2H), 3.42 (t, *J* = 2.4 Hz, 2H), 3.30 (d, *J* = 2.4 Hz, 2H). <sup>13</sup>C NMR (100 MHz, DMSO-*d*<sub>6</sub>) δ 160.3, 146.4, 144.6, 142.8, 133.9, 130.1, 128.5 (q, <sup>2</sup>*J*<sub>C-F</sub> = 94.9), 124.7 (d, <sup>1</sup>*J*<sub>C-F</sub> = 270.2), 125.7 (d, <sup>4</sup>*J*<sub>C-F</sub> = 3.7), 114.6, 78.0, 77.9, 56.9, 54.1, 43.5, 42.1. HRMS (ESI): *m/z* calcd for C<sub>18</sub>H<sub>18</sub>F<sub>3</sub>N<sub>2</sub>O<sub>2</sub> [M + H]<sup>+</sup>: 351.1315 found 351.1318 HPLC purity: 99.13%.

#### 4.9.14. 2-(((3,5-Difluorobenzyl)(prop-2-yn-1-yl)amino)methyl)-5-hydroxy-1-methylpyridin-4(1H)-one (14n)

Yield: 86%, White solid, m.p. 182.8–184.6 °C, <sup>1</sup>H NMR (400 MHz, DMSO-*d*<sub>6</sub>) δ 11.16 (br, 1H), 8.30 (s, 1H), 7.42 (s, 1H), 7.17–7.09 (m, 1H), 7.09–7.02 (m, 2H), 4.04 (s, 3H), 3.87 (s, 3H), 3.73 (s, 2H), 3.39 (t, *J* = 2.4 Hz, 1H), 3.31 (d, *J* = 2.4 Hz, 2H). <sup>13</sup>C NMR (100 MHz, DMSO-*d*<sub>6</sub>) δ 162.8 (dd, <sup>1</sup>*J*<sub>C-F</sub> = 244.8, <sup>3</sup>*J*<sub>C-F</sub> = 13.2), 160.3, 146.3, 144.6, 142.8 (t, <sup>3</sup>*J*<sub>C-F</sub> = 9.0 Hz), 134.0, 114.6, 112.2 (dd, <sup>2</sup>*J*<sub>C-F</sub> = 24.8 Hz), 103.4 (t, <sup>2</sup>*J*<sub>C-F</sub> = 51.2), 80.3, 77.9, 56.7, 54.0, 43.5, 42.1. HRMS (ESI): *m/z* calcd for C<sub>17</sub>H<sub>17</sub>F<sub>2</sub>N<sub>2</sub>O<sub>2</sub> [M + H]<sup>+</sup>: 319.1253 found 319.1256 HPLC purity: 99.94%.

#### 4.10. Determination of pK<sub>a</sub> and Fe<sup>3+</sup> affinity by spectrophotometry

The method of this experiment had been published in the previous work [38]. Please refer to S2 for specific experiment plan.

#### 4.11. Determination of monoamine oxidase activity and selectivity calculation

The method of this experiment had been published in the previous work [38]. Please refer to S3 for specific experiment plan.

#### 4.12. Permeability predictions of BBB permeability based on data platforms

To improve the accuracy and credibility of the final prediction results, three data platforms (ADMETlab, SwissADME, admetSAR) were selected for investigation.

ADMETlab (<http://admet.scbdd.com/>) is a widely used, user-friendly free web platform. The platform is based on a database (288,967 entries). The platform contains four functional modules for drug similarity analysis, ADMET endpoint prediction, systematic evaluation and similarity search to achieve rapid compound screening [44].

The SwissADME platform (<http://www.swissadme.ch>) provides free access to a series of accurate prediction models to calculate physicochemical properties, drug-likeness and medicinal chemistry friendliness, including internally proficient methods. Finally, the key parameters of the molecular collection can be quickly predicted [45].

admetSAR 2.0 is a free platform for predicting the ADMET properties of drug candidates (<http://www.admetexp.org>). These models are continuously optimized by training with the most advanced machine learning methods, including support vector machines. The entire dataset was collected from Wang and co-workers. This reliable classification model was built by machine learning ways and resampling methods [46].

#### 4.13. PAMPA-BBB assay

The test compound and the commercial drugs were dissolved in DMSO at 5 mg/mL and then diluted with phosphate buffer saline (PBS) buffer solution (PH = 7.4) into a 25 µg/mL solution to be tested. An appropriate amount of porcine polar brain lipid (PBL) was solubilized directly in dodecane at a concentration of 20 mg/mL solution. The PBL used in this assay was purchased from Avanti Polar Lipids, Inc. The prepared PBL solution was added to the filter surface of the donor plate (4 µL per well), after the entire filter membrane (area = 0.28 cm<sup>2</sup>) was impregnated with the PBL, the test compound solution (V<sub>d</sub>) was added to the donor plate (150 µL), and the acceptor well was filled with 300 µL of PBS buffer (V<sub>a</sub>). The donor plate was carefully put on the acceptor plate so that the membrane and the upper and lower liquid levels were in contact with each other. Afterward, the lid was covered and stood for 6 h in the dark and constant temperature at 25 °C. The concentration of the drug in the acceptor, the donor, and the reference wells was determined by the microplate reader. According to the Pe Eq. (1), the concentration of the compound in the hole, and the permeability could be calculated (the concentration of the compound is calculated by substituting the UV absorbance into the standard curve, and each group of samples is tested in parallel 8 times). The concentration-absorbance standard curve of each compound can be found in the S3 [43,47,48].

$$Pe = \left\{ C \times -\ln \left( 1 - \frac{n_{\text{acceptor}}}{n_{\text{total}}} \right) \right\} \text{ where } C = \left( V_d \times \frac{V_a}{\text{Area} \times \text{time} \times (V_d + V_a)} \right) \quad (1)$$

#### 4.14. Behavioral research

ICR mice (20–25 g, female) were ordered from the Zhejiang Academy of Medical Sciences (Hangzhou, China). The test protocol was reviewed and approved by the Animal Welfare and Ethics Committee of Zhejiang University of Technology. Intraperitoneal injection was selected as the route of administration for this test, and the injection vehicle was phosphate-buffered saline. Pargyline (the positive drug) and scopolamine hydrobromide (the modeling drug) were supplied by Aladdin Reagents.

The mice were purchased and raised in the animal center for seven days to eliminate environmental stress. All mice were divided equally: (i) control, (ii) model, (iii) pargyline + scopolamine (positive group), and (iv) compound 6b + scopolamine [49]. The dosage of the compounds was 15 mg/kg. Over fifteen days, the frequency of

administration was once a day, and the administration time was fixed.

From the tenth day to the fifteenth day, the behavioral tests were conducted. The maze (120 cm in diameter and 60 cm high) was in a dark room and consisted of four quadrants. Mice were trained once in each of the four quadrants of the pool (days 10–14), each time for 120 s, and the time that it took for the mice to find the platform was recorded. Regardless of whether the mice successfully reach the platform within 120 s, they must remain on the platform for 10 s. On the 15th day, the platform was evacuated, and the mice received an exploratory experiment from the second quadrant. The distance the mice traveled before reaching the platform for the first time, the number of times the mice crossed the platform and the time of escape latency were recorded with Panlab SMART 3.0 and processed with GraphPad Prism 6 software.

### Declaration of Competing Interest

The authors declare that they have no known competing financial interests or personal relationships that could have appeared to influence the work reported in this paper.

### Acknowledgements

This project was supported by the Zhejiang Key R&D Program (No. 2021C03085); National Natural Science Foundation of China, NSFC (Grant No. 21978273, 21576239 and 81803340) and Zhejiang Natural Science Foundation (LY20H300004).

### Appendix A. Supplementary material

Supplementary data to this article can be found online at <https://doi.org/10.1016/j.bioorg.2021.105013>.

### References

- Alzheimer's Disease International, World Alzheimer Report 2019 Attitudes to dementia, <https://www.alz.co.uk/research/world-report-2019>.
- L.E. Hebert, J. Weuve, P.A. Scherr, D. A. Evans, Alzheimer disease in the United States (2010–2050) estimated using the 2010 census, *Neurology*. 80 (2013) 1778–1783.
- L.F. Jia, M. Quan, Y. Fu, T. Zhao, Y. Li, C.B. Wei, Y. Tang, Q. Qin, F. Wang, Y. Qing, S.L. Shi, Y.J. Wang, Y.F. Du, J.W. Zhang, J.J. Zhang, B.Y. Luo, Q.M. Qu, C.K. Zhou, S. Gauthier, J.P. Jia, Dementia in China: epidemiology, clinical management, and research advances, *Lancet Neurol.* 19 (2020) 81–92.
- R. Cimler, P. Maresova, J. Kuhnova, K. Kuca, Predictions of Alzheimer's disease treatment and care costs in European countries, *PLoS ONE* 14 (2019), e0210958.
- E. Karran, M. Mercken, B. De Strooper, The amyloid cascade hypothesis for Alzheimer's disease: an appraisal for the development of therapeutics, *Nat. Rev. Drug Discov.* 10 (2011) 698–712.
- P. Scheltens, K. Blennow, M.M.B. Breteler, B. de Strooper, G.B. Frisoni, S. Salloway, W.M. Van der Flier, Alzheimer's disease, *Lancet* 388 (2016) 501–517.
- M.G. Savelieff, G. Nam, J. Kang, H.J. Lee, M. Lee, M.H. Lim, Development of multifunctional molecules as potential therapeutic candidates for Alzheimer's disease, Parkinson's disease, and amyotrophic lateral sclerosis in the last decade, *Chem. Rev.* 119 (2019) 1221–1322.
- Alzheimer's Association. 2020 Alzheimer's disease facts and figures, *Alzheimer's Dementia* 16 (2020) 391–460.
- S. Srivastava, R. Ahmad, S.K. Khare, Alzheimer's disease and its treatment by different approaches: A review, *Eur. J. Med. Chem.* 216 (2021), 113320.
- J.S. Lan, Y. Ding, Y. Liu, P. Kang, J.W. Hou, X.Y. Zhang, S.S. Xie, T. Zhang, Design, synthesis and biological evaluation of novel coumarin-N-benzyl pyridinium hybrids as multi-target agents for the treatment of Alzheimer's disease, *Eur. J. Med. Chem.* 139 (2017) 48–59.
- L. Zhang, P. Zhao, C. Yue, Z. Jin, Q. Liu, X. Du, Q. He, Sustained release of bioactive hydrogen by Pd hydride nanoparticles overcomes Alzheimer's disease, *Biomaterials* 197 (2019) 393–404.
- A.C. Tripathi, S. Upadhyay, S. Paliwal, S.K. Saraf, Privileged scaffolds as MAO inhibitors: Retrospect and prospects, *Eur. J. Med. Chem.* 145 (2018) 445–497.
- M. do Carmo Carrreiras, L. Ismaili, J. Marco-Contelles, Propargylamine-derived multi-target directed ligands for Alzheimer's disease therapy, *Bioorg. Med. Chem. Lett.* 30 (2020) 126880.
- B.P. Kennedy, M.G. Ziegler, M. Alford, L.A. Hansen, L.J. Thal, E. Masliah, Early and persistent alterations in prefrontal cortex MAO A and B in Alzheimer's disease, *J. Neural Transm.* 110 (2003) 789–801.
- S. Carradori, R. Silvestri, New frontiers in selective human MAO-B inhibitors, *J. Med. Chem.* 58 (2015) 6717–6732.
- C.A. Cobb, M.P. Cole, Oxidative and nitrate stress in neurodegeneration, *Neurobiol. Dis.* 84 (2015) 4–21.
- M. Yogeve-Falach, T. Amit, O. Bar-Am, M.B.H. Youdim, The importance of propargylamine moiety in the anti-Parkinson drug rasagiline and its derivatives for MAPK-dependent amyloid precursor protein processing, *FASEB J.* 17 (2003) 2325–2327.
- M. Naoi, W. Maruyama, H. Yi, Y. Akao, Y. Yamaoka, M. Shamoto-Nagai, Neuroprotection by propargylamines in Parkinson's disease: intracellular mechanism underlying the anti-apoptotic function and search for clinical markers, *J. Neural Transm. Suppl.* 72 (2007) 121–131.
- M.B.H. Youdim, The path from anti Parkinson drug Selegiline and Rasagiline to multifunctional neuroprotective anti Alzheimer drugs Ladostigil and M30, *Curr. Alzheimer Res.* 3 (2006) 541–550.
- O. Bar-Am, T. Amit, M.B.H. Youdim, Aminoindan and hydroxyaminoindan, metabolites of rasagiline and ladostigil, respectively, exert neuroprotective properties in vitro, *J. Neurochem.* 103 (2007) 500–508.
- T. Amit, O. Bar-Am, D. Mechlovich, L. Kupersmidt, M.B.H. Youdim, O. Weinreb, The novel multitarget iron chelating and propargylamine drug M30 affects APP regulation and processing activities in Alzheimer's disease models, *Neuropharmacology* 123 (2017) 359–367.
- D. Arduino, D. Silva, S.M. Cardoso, S. Chaves, C.R. Oliveira, M.A. Santos, New hydroxypyridinone iron-chelators as potential anti-neurodegenerative drugs, *Front. Biosci.* 13 (2008) 6763–6774.
- L. Wang, G. Esteban, M. Ojima, O.M. Bautista-Aguilera, T. Inokuchi, I. Moraleda, I. Iriepa, A. Samadi, M.B.H. Youdim, A. Romero, E. Soriano, R. Herrero, A. P. Fernández Fernández, J. Ricardo-Martínez-Murillo, M. Unzeta Marco-Contelles, Donepezil + propargylamine + 8-hydroxyquinoline hybrids as new multifunctional metal-chelators, ChE and MAO inhibitors for the potential treatment of Alzheimer's disease, *Eur. J. Med. Chem.* 80 (2014) 543–561.
- E. Mezeiova, J. Janockova, R. Andrys, O. Soukup, T. Kobrova, L. Muckova, J. Pejchal, M. Simunkova, J. Handl, P. Micankova, J. Capek, T. Rousar, M. Hrabivova, E. Nepovimova, J.L. Marco-Contelles, M. Valko, J. Korabecny, 2-Propargylamino-naphthoquinone derivatives as multipotent agents for the treatment of Alzheimer's disease, *Eur. J. Med. Chem.* 211 (2021), 113112.
- X.Y. Jiang, T. Zhou, R.R. Bai, Y.Y. Xie, Hydroxypyridinone-based iron chelators with broad-ranging biological activities, *J. Med. Chem.* 63 (2020) 14470–14501.
- S. Niksresht, A.I. Bush, S. Aytton, Treating Alzheimer's disease by targeting iron, *Brit. J. Pharmacol.* 176 (2019) 3622–3635.
- N. Spoto, J. Acosta-Cabrero, E. Stomrud, B. Lampinen, O.T. Strandberg, D. van Westen, O. Hansson, Relationship between cortical iron and tau aggregation in Alzheimer's disease, *Brain* 143 (2020) 1341–1349.
- M. Bulik, B. Kenkhuus, L.M. van der Graaf, J.J. Goeman, R. Natté, L. van der Weerd, Postmortem T2\*-weighted MRI imaging of cortical iron reflects severity of Alzheimer's disease, *J. Alzheimers Dis.* 65 (2018) 1125–1137.
- C. Cheignon, M. Tomas, D. Bonnefont-Rousselot, P. Faller, C. Hureau, F. Collin, Oxidative stress and the amyloid beta peptide in Alzheimer's disease, *Redox Biol.* 14 (2018) 450–464.
- M.A. Greenough, J. Camakaris, A.I. Bush, Metal dyshomeostasis and oxidative stress in Alzheimer's disease, *Neurochem. Int.* 62 (2013) 540–555.
- R.C. Hider, S. Singh, J.B. Porter, E.R. Huehns, The development of hydroxypyridinone-ones as orally active iron chelators, *Ann. N. Y. Acad. Sci.* 612 (1990) 327–338.
- W.T. Chen, X. Yuan, Z. Li, Z.D. Lu, S.S. Kong, H.D. Jiang, H.B. Du, X.H. Pan, M. Nandi, X.L. Kong, K. Brown, Z.D. Liu, G.L. Zhang, R.C. Hider, Y.P. Yu, CN128: A new orally active hydroxypyridinone iron chelator, *J. Med. Chem.* 63 (2020) 4215–4226.
- P. Xu, M.K. Zhang, R. Sheng, Y.M. Ma, Synthesis and biological evaluation of deferiprone-resveratrol hybrids as antioxidants, A $\beta_{1-42}$  aggregation inhibitors and metal-chelating agents for Alzheimer's disease, *Eur. J. Med. Chem.* 127 (2017) 174–186.
- J.T. Zhou, X.Y. Jiang, S.Y. He, H.L. Jiang, F. Feng, W.Y. Liu, W. Qu, H.P. Sun, Rational design of multitarget-directed ligands: strategies and emerging paradigms, *J. Med. Chem.* 62 (2019) 8881–8914.
- O. Benek, J. Korabecny, O. Soukup, A perspective on multi-target drugs for Alzheimer's disease, *Trends Pharmacol. Sci.* 41 (2020) 434–445.
- X.Y. Jiang, J.N. Guo, Y.J. Lv, C.S. Yao, C.J. Zhang, Z.S. Mi, Y. Shi, J.P. Gu, T. Zhou, R.R. Bai, Y.Y. Xie, Rational design, synthesis and biological evaluation of novel multitargeting anti-AD iron chelators with potent MAO-B inhibitory and antioxidant activity, *Bioorgan. Med. Chem.* 28 (2020), 115550.
- C.J. Zhang, K. Yang, S.H. Yu, J. Su, S.J. Yuan, J.X. Han, Y. Chen, J.P. Gu, T. Zhou, R. Bai, Y.Y. Xie, Design, synthesis and biological evaluation of hydroxypyridinonecoumarin hybrids as multimodal monoamine oxidase B inhibitors and iron chelates against Alzheimer's disease, *Eur. J. Med. Chem.* 180 (2019) 367–382.
- J.N. Guo, Z.S. Mi, X.Y. Jiang, C.J. Zhang, Z.L. Guo, L.Z. Li, J.P. Gu, T. Zhou, R. Bai, Y.Y. Xie, Design, synthesis and biological evaluation of potential anti-AD hybrids with monoamine oxidase B inhibitory and iron-chelating effects, *Bioorg. Chem.* 108 (2021), 104564.
- Z.S. Mi, B. Gan, S.H. Yu, J.N. Guo, C.J. Zhang, X.Y. Jiang, T. Zhou, R.R. Bai, Y. Xie, Dual-target anti-Alzheimer's disease agents with both iron ion chelating and monoamine oxidase-B inhibitory activity, *J. Enzyme Inhib. Med. Chem.* 34 (2019) 1489–1497.
- D. Hazarika, A.J. Borah, P. Phukan, Facile, catalyst-free cascade synthesis of sulfonyl guanidines via carbodiimide coupling with amines, *Chem. Commun.* 55 (2019) 1418–1421.
- Y.Y. Xie, Z.D. Lu, X.L. Kong, T. Zhou, S. Bansal, R. Hider, Systematic comparison of the mono-, dimethyl- and trimethyl 3-hydroxy-4(1H)-pyridones e Attempted

- optimization of the orally active iron chelator, deferiprone, *Eur. J. Med. Chem.* 115 (2016) 132–140.
- [42] L. F. N. Lemes, G. de Andrade Ramos, A. S. de Oliveira, F. M. R. da Silva, G. de Castro Couto, M. da Silva Boni, M. J. R. Guimarães, I. N. O. Souza, M. Bartolini, V. Andrisano, P. C. do Nascimento Nogueira, E. R. Silveira, G. D. Brand, O. Soukup, J. Korábecný, N. C. Romeiro, N. G. Castro, M. L. Bolognesi, L. A. S. Romeiro, Cardanol-derived AChE inhibitors: Towards the development of dual binding derivatives for Alzheimer's disease, *Eur. J. Med. Chem.* 108 (2016) 687–700.
- [43] L. Di, E.H. Kerns, K. Fan, O.J. McConnell, G.T. Carter, High throughput artificial membrane permeability assay for blood/brain barrier, *Eur. J. Med. Chem.* 38 (2003) 223–232.
- [44] J. Dong, N.N. Wang, Z.J. Yao, L. Zhang, Y. Cheng, D.F. Ouyang, A.P. Lu, D.S. Cao, ADMETlab: a platform for systematic ADMET evaluation based on a comprehensively collected ADMET database, *J. Cheminform.* 10 (2018) 29.
- [45] A. Daina, O. Michielin, V. Zoete, SwissADME: a free web tool to evaluate pharmacokinetics, drug-likeness and medicinal chemistry friendliness of small molecules, *Sci. Rep.* 7 (2017) 42717.
- [46] F.X. Cheng, W.H. Li, Y.D. Zhou, J. Shen, Z.R. Wu, G.X. Liu, P.W. Lee, Y. Tang, admetSAR: A comprehensive source and free tool for assessment of chemical ADMET properties, *J. Chem. Inf. Model.* 52 (2012) 3099–3105.
- [47] V. Hepnarova, J. Korabecny, L. Matouskova, P. Jost, L. Muckova, M. Hrabnova, N. Vykoukalova, M. Kerhartova, T. Kucera, R. Dolezal, E. Nepovimova, K. Spilovska, E. Mezeiova, N.L. Pham, D. Jun, F. Staud, D. Kaping, K. Kuca, O. Soukup, The concept of hybrid molecules of tacrine and benzyl quinolone carboxylic acid (BQCA) as multifunctional agents for Alzheimer's disease, *Eur. J. Med. Chem.* 150 (2018) 292–306.
- [48] Q.H. Liu, J.J. Wu, F. Li, P. Cai, X.L. Yang, L.Y. Kong, X.B. Wang, Synthesis and pharmacological evaluation of multi-functional homoisoflavonoid derivatives as potent inhibitors of monoamine oxidase B and cholinesterase for the treatment of Alzheimer's disease, *Med. Chem. Commun.* 8 (2017) 1459–1467.
- [49] Y. Chen, H.Z. Lin, J. Zhu, K. Gu, Q. Li, S.Y. He, X. Lu, R.X. Tan, Y.Q. Pei, L. Wu, Y. Y. Bian, H.P. Sun, Design, synthesis, in vitro and in vivo evaluation of tacrine–cinnamic acid hybrids as multi-target acetyl- and butyrylcholinesterase inhibitors against Alzheimer's disease, *RSC Adv.* 7 (2017) 33851–33867.